



HAL
open science

Insights into Cisplatin Binding to Uracil and Thiouracils from IRMPD Spectroscopy and Tandem Mass Spectrometry

Maria Elisa Crestoni, Davide Corinti, Barbara Chiavarino, Simonetta
Fornarini, Debora Scuderi, Jean-Yves Salpin

► **To cite this version:**

Maria Elisa Crestoni, Davide Corinti, Barbara Chiavarino, Simonetta Fornarini, Debora Scuderi, et al.. Insights into Cisplatin Binding to Uracil and Thiouracils from IRMPD Spectroscopy and Tandem Mass Spectrometry. *Journal of The American Society for Mass Spectrometry*, 2020, 31 (4), pp.946-960. 10.1021/jasms.0c00006 . hal-02533691

HAL Id: hal-02533691

<https://hal.science/hal-02533691>

Submitted on 6 Apr 2020

HAL is a multi-disciplinary open access archive for the deposit and dissemination of scientific research documents, whether they are published or not. The documents may come from teaching and research institutions in France or abroad, or from public or private research centers.

L'archive ouverte pluridisciplinaire **HAL**, est destinée au dépôt et à la diffusion de documents scientifiques de niveau recherche, publiés ou non, émanant des établissements d'enseignement et de recherche français ou étrangers, des laboratoires publics ou privés.

1
2
3 **Insights into Cisplatin Binding to Uracil and Thiouracils from IRMPD**
4 **Spectroscopy and Tandem Mass Spectrometry**
5
6
7
8
9

10 Davide Corinti¹, Maria Elisa Crestoni*¹, Barbara Chiavarino¹, Simonetta Fornarini¹, Debora
11 Scuderi,² and Jean-Yves Salpin*^{3,4}
12
13

14
15
16 1) Dipartimento di Chimica e Tecnologie del Farmaco, Università di Roma “La Sapienza”, P.le A.
17 Moro 5, 00185 Roma, ITALY

18
19 2) Université Paris-Saclay, CNRS, Institut de Chimie Physique UMR8000, 91405, Orsay, France

20
21 3) Université Paris-Saclay, CNRS, Univ Evry, LAMBE, Evry-Courcouronnes, 91025, France

22
23 4) CY Cergy Paris Université, LAMBE, Evry-Courcouronnes, 91025, France
24
25
26
27

28 **Corresponding Authors:**

29
30 mariaelisa.crestoni@uniroma1.it (M.E.C.)

31
32 jeanyves.salpin@univ-evry.fr (J.-Y.S.)
33
34
35
36
37
38
39
40
41
42
43
44
45
46
47
48
49
50
51
52
53
54
55
56
57
58
59
60

Abstract.

The monofunctional primary complexes *cis*-[PtCl(NH₃)₂(L)]⁺, formed by the reaction of cisplatin, a major chemotherapeutic agent, with four nucleobases L, i.e. uracil (U), 2-thiouracil (2SU), 4-thiouracil (4SU) and 2,4-dithiouracil (24dSU), have been studied by a combination of infrared multiple photon dissociation (IRMPD) action spectroscopy, in both the fingerprint (900-1900 cm⁻¹) and the N-H/O-H stretching (3000-3800 cm⁻¹) ranges, energy-resolved collision-induced dissociation (CID) mass spectrometry and by density functional calculations at the B3LYP/LACVP/6-311G** level. On the basis of the comparison across the experimental features and the linear IR spectra of conceivable structures, the cisplatin residue is found to promote a monodentate interaction preferentially with the O4(S4) atoms of the canonical forms of U, 4SU and 24dSU and to the S2 atom of 2SU, yielding the most stable structures. Additional absorptions reveal the presence of minor, alternative tautomers in the sampled ion populations of 2SU and 24dSU, underlying the ability of cisplatin to increase the prospect of (therapeutically beneficial) nucleic acid strand disorder. Implication of these evidences may provide insights into drug mechanism and design.

Keywords: Cisplatin, Uracil, Thiouracils, IRMPD spectroscopy, FT-ICR mass spectrometry

INTRODUCTION

In spite of their peculiar biological properties, only a few theoretical and experimental studies dedicated to the structural characterization of thiouracils at the molecular level were available at the end of the eighties. However, these molecules have since attracted significant attention. Thiouracils have been identified as minor components of transfer-RNA[1], and the existence of these molecules in many tautomeric forms, like for other nucleobases, seems to be a key point to account for the mistranslation of genetic information[2-4]. Therefore, this feature has motivated both theoretical and experimental studies on tautomeric equilibria of nucleobases and thiobases, in order to establish a relationship between the presence of enol tautomeric forms and the appearance of point mutations during DNA replication [5-16]. In addition, thiouracils exhibit many interesting therapeutic applications for antithyroid [17, 18], antiviral [19, 20], anticancer [21, 22] and heart disease [23, 24] therapies.

Due to the presence of soft thiocarbonyl group(s), thiouracils have also been selected to reveal and capture transition metal ions and notably mercury [25, 26]. However, despite strong and selective binding properties, gas-phase studies describing their interactions with metal ions at the molecular level are rather scarce. The effect of Cu^{2+} ions onto deprotonated forms of thiouracils has been inspected only theoretically [27, 28], whereas the scrutiny of Pb^{2+} /thiouracils [29] and Ca^{2+} /thiouracils [30, 31] complexes combined both experiments and calculations. More recently, Infrared Multiple Photon Dissociation (IRMPD) spectroscopy has been applied to the characterization of protonated and sodiated uracil and thiouracils complexes [15, 32, 33], disclosing that protonation preferentially stabilizes alternative, noncanonical tautomers of uracil and of all the thiouracils aside from 4-thiouracil (4SU), whereas the sodium cation binds to the canonical tautomers of uracil (U) and 2-thiouracil (2SU), and to minor tautomers of 4-thiouracil (4SU) and 2,4-thiouracil (24SU). Other contributions on the binding of Cu^+ /uracil and Ag^+ /uracil,[34] aimed at determining if tautomeric forms and cation- π binding that may cause mismatch are involved in the

1
2
3 complexation process, have been reported. Proceeding with growing complexity of the ligand,
4
5 IRMPD spectra of protonated thiated uridines have been recently scrutinized unveiling the
6
7 occurrence of protonation on the 4 position of hydroxyl-sulfhydryl or sulfhydryl-hydroxyl
8
9 tautomeric structures [35].

10
11
12 In the context of the ongoing interest in spectroscopic surveys on naked primary aqua intermediates
13
14 [36] of cisplatin (*cis*-diamminedichloroplatinum(II)), a leading antitumor agent which has
15
16 revolutionized cancer treatments, and on its complexes with prime targets including amino acids
17
18 [37-39], purines [40] and nucleotides [41, 42], a thorough description of cisplatin (cisPt) interaction
19
20 with uracil (U), and its thio-derivatives, namely 2-thiouracil (2SU), 4-thiouracil (4SU) and 2,4-
21
22 dithiouracil (24dSU), is presented here based on mass spectrometry, IRMPD spectroscopy and
23
24 density functional calculations.

25
26
27
28 Our previous work on cisplatin binding to adenine and guanine [40] has shown that Pt is attached to
29
30 the N7 position of guanine and to the N3 and N1 atoms of adenine. Analogous coordination modes
31
32 besides a macrochelate arrangement have emerged in the spectroscopic scrutiny of the cisPt adducts
33
34 with the nucleic acid building blocks, 2'-deoxyguanosine-5'monophosphate [41] and 2'-
35
36 deoxyadenosine-5'monophosphate [42].

37
38
39 Here, the presence of N, O and S donor atoms in thiouracils may enlarge the variety of cisPt
40
41 coordination targets. The present study aims to obtain a direct experimental characterization of *cis*-
42
43 $[\text{PtCl}(\text{NH}_3)_2(\text{L})]^+$ ions, accessed by electrospray ionization (ESI), so as to identify the preferred
44
45 metal binding site, to define the various (non)canonical tautomeric forms of uracil and three
46
47 thiouracils (L=2SU, 4SU, 24dSU), and to elucidate the effect of thio-keto substitution onto the
48
49 complexation process.

50
51
52
53 Unveiling the intrinsic properties of metal-containing therapeutics may contribute to elucidate their
54
55 mechanisms of actions and to spur new directions in the design of anticancer drugs [43].
56
57
58
59
60

EXPERIMENTAL SECTION

Materials. Cisplatin, uracil and thiouracils were purchased from Sigma-Aldrich (Sigma-Aldrich s.r.l. Milan, Italy) and used without further purification. To generate the complexes of interest, an aqueous solution of cisplatin ca. 1×10^{-3} M, allowed to stand overnight, was mixed with a solution of the selected (thio)uracil nucleobases (L= U, 2SU, 4SU, 24dSU) and diluted with water. Final solutions of the two analytes in isomolar ratio and concentration of 5×10^{-5} M in methanol/water (1:1 v/v) were infused into the ESI source.

CID Experiments. Energy-variable collision induced dissociation (CID) experiments have been recorded on a commercial hybrid triple-quadrupole linear ion trap mass spectrometer (2000 Q-TRAP Applied Biosystems), with a Q1q2Q_{LIT} configuration (Q1, first mass analyzing quadrupole ; q2, nitrogen-filled collision cell ; Q_{LIT}, linear ion trap) equipped with an ESI source. After desolvation, electrosprayed [*cis*-[PtCl(NH₃)₂(L)]⁺ ions were mass-selected (Q1) and allowed to collide with N₂ (nominal pressure of 1.1×10^{-5} mbar) in q2 at variable collision energy ($E_{\text{LAB}} = 5\text{-}50$ eV). The product ions were monitored by scanning Q_{LIT}. Typical experimental parameters were : Ion Spray Voltage at 5500 V, Curtain Gas set at 20 psi, GS1 at 20 psi, Declustering Potential at 40 V and Entrance Potential at 5 V. Quantitative absolute threshold energies are by no means directly amenable. However, phenomenological dissociation threshold energies (TEs) and comparative assessment for different fragmentation channels can be attained from the linear interpolation of the rise of breakdown curves by converting the collision energies to the center of mass frame $E_{\text{CM}} = [m/(m + M)]E_{\text{LAB}}$, where m and M are the masses of the collision gas and of the ion, respectively. Corrections for the nominal zero energy were acquired from retarding potential (RP) experiments, in which the intensity of the parent ion is plotted as a function of the entrance potential [44].

1
2
3 **IRMPD Experiments.** IRMPD experiments were performed in two distinct energy ranges. The
4 vibrational modes associated with the XH (X = C, N, O) stretches in the 3100-3800 cm⁻¹ frequency
5 range were recorded by means of an optical parametric oscillator/amplifier (OPO/OPA,
6 LaserVision) laser system coupled to a Paul ion trap mass spectrometer (Esquire 6000+, Bruker
7 Daltonics), as already described [45,46]. The typical output energy from the OPO/OPA laser
8 operated at 10 Hz was 20-24 mJ/pulse, with a spectral bandwidth of about 3-4 cm⁻¹. In the trap, ions
9 were accumulated for 10 ms and then mass-selected prior to IR irradiation for 500 ms. The mass
10 spectrum was typically derived from an accumulation of four scans. To improve the IRMPD signal
11 intensity, the sampled ions were irradiated by using an auxiliary, CO₂ laser (Universal Laser
12 Systems, Inc., Scottsdale, AZ, USA). A 20 ms long CO₂ pulse of 13 W, corresponding to an energy
13 of 260 mJ, followed each OPO/OPA pulse, delayed by 10 μs [47].

14
15
16
17
18
19
20
21
22
23
24
25
26
27
28
29 The fingerprint region (800-2000 cm⁻¹) was explored using the beamline of the free electron laser
30 (FEL) of the Centre Laser Infrarouge d'Orsay (CLIO) [48, 49]. The electron energy of the FEL was
31 set at 44.4 MeV to optimize the laser power in the frequency region of interest and ensure a fairly
32 stable laser power (900-1100 mW). IR light was delivered in 9 μs macropulses (25 Hz), each
33 containing 600 micropulses (0.5–3 ps long). Typical macropulse energies are ca. 40 mJ. For the
34 present study, the FEL beamline was admitted into the cell of with a hybrid FT-ICR tandem mass
35 spectrometer (APEX-Qe Bruker) equipped with a 7.0 T actively shielded magnet and coupled to a
36 quadrupole-hexapole interface for mass-filtering and ion accumulation. The complexes of interest
37 were first mass-selected in the quadrupole and then accumulated and collisionally cooled for 300
38 ms in the presence of a buffer gas (Argon) in the linear hexapole, prior to their transfer into the ICR
39 cell. Isolated charged complexes were then irradiated for 250-500 ms with the IR FEL light, after
40 which the resulting ions are mass-analyzed [49, 50]. To avoid saturation effects of the most intense
41 absorptions, IRMPD spectra were also recorded using one attenuator to decrease the irradiation
42 power by a factor of three.

1
2
3 The IRMPD spectra presently reported correspond to the photofragmentation yield R ($R = -$
4 $\ln[I_{\text{precursor}}/(I_{\text{precursor}} + \sum I_{\text{fragment}})]$, where $I_{\text{precursor}}$ and I_{fragment} are the integrated intensities of the mass
5 peaks of the precursor and of the fragment ions, respectively) as a function of the photon
6 wavenumber [49, 51].
7
8
9
10

11 **Computational Studies.** Density functional calculations were carried out using the hybrid B3LYP
12 density functional [52, 53], as implemented in the Gaussian-09 set of programs [54]. Geometry
13 optimization was achieved without any symmetry constraint, using the 6-311G** basis set. In order
14 to describe the Pt atom, we combined the Los Alamos effective core potential (ECP) with the
15 LACV3P** basis set [55-57]. Harmonic vibrational frequencies were also computed at this level to
16 estimate the zero-point vibrational energy (ZPE) corrections and to characterize the stationary
17 points as local minima or saddle points.
18
19
20
21
22
23
24
25
26
27

28 The infrared absorption spectra of the various structures were calculated within the harmonic
29 approximation. Calculated frequencies were scaled by a factor of 0.974 in the fingerprint region and
30 by 0.957 in the X-H stretch region, for a better agreement with the experimental spectrum, as
31 detailed in a previous study about the *cis*-[PtCl(NH₃)₂G]⁺ complex [40].
32
33
34
35
36
37

38 **Results and Discussion**

39
40
41 **Photodissociation and CID Experiments.** A great deal of effort has been devoted so far in
42 examining the stability and binding interactions of uracil and its thio- and halo-derivatives by means of
43 energy-resolved CID experiments [29, 58-61] and chemical dynamics simulations [62,63] and
44 statistical reactivity approaches [64].
45
46
47
48
49

50 Here, the complexes of cisplatin with uracil and thiouracil nucleobases, *cis*-[Pt(CH₃)₂Cl(L)]⁺ (L=U,
51 2SU, 4SU, 24dSU) were mass isolated and submitted to CID to obtain information about structural and
52 thermodynamic features. The observed fragments are reported in Table 1 together with the values of
53 phenomenological dissociation threshold (TE) obtained from breakdown curves. Overall, the four
54
55
56
57
58
59
60

1
2
3 complexes present a similar dissociation pattern involving mainly the ammonia ligands and the
4 remaining chlorido ligand eliminated as hydrogen chloride. The complexes presenting either U, 2SU
5 or 4SU as ligands give two additional fragmentation pathways, including the loss of NHCO, which
6 originates from the fragmentation of the nucleobase ring, and the elimination of the corresponding
7 neutral nucleobase (m/z 263), likely by direct cleavage of the L-Pt bond. However, the latter
8 fragmentation is much more prevalent for *cis*-[PtCl(NH₃)₂(U)]⁺, in which case this channel represents
9 one of the most abundant dissociation path even at low collision energy (Figure 1). Indeed, the lower
10 percentage of intact 2SU and 4SU cleavage from the corresponding *cis*Pt complexes, as well as the
11 absence of the corresponding dissociation path from *cis*-[PtCl(NH₃)₂(24dSU)]⁺ (Figures S1-3) are in
12 agreement with the well-known bias for Pt binding to S-containing nucleophiles, which increases the
13 energetic demand for breaking the Pt-L bond [43].

14
15
16
17
18
19
20
21
22
23
24
25
26
27
28
29
30
31
32
33
34
35
36
37
38
39
40
41
42
43
44
45
46
47
48
49
50
51
52
53
54
55
56
57
58
59
60
The breakdown curves together with the RP experiments are reported in Figure S4-6 in the SI, with the
exception of the *cis*-[PtCl(NH₃)₂(U)]⁺ complex, whose low absolute intensity hampered obtaining
meaningful data. The phenomenological TE values for the remaining complexes were found to be
equal to 89 ± 10 -15, 89 ± 10 -15 and 75 ± 10 -15 kJ mol⁻¹ for 2SU, 4SU and 24dSU, respectively. These
values, obtained by summing the abundances of all fragments, allow a comparative evaluation for the
lowest energy dissociation route, namely the cleavage of ammonia in the *trans* position with either the
chlorido or the nucleobase ligand. In four-coordinate planar complexes, the threshold energy for
breaking a metal-ligand bonds is influenced by the nature of the ligand *trans* to the leaving group. As a
result, the same TE values obtained for 2SU and 4SU complexes, which therefore are barely
differentiated by CID measurements, suggest these nucleobases bind platinum rather strongly and at a
site with akin electronic features. The slightly smaller TE value (by 14 kJ mol⁻¹) observed for *cis*-
[PtCl(NH₃)₂(24dSU)]⁺ is consistent with 24dSU interacting in a similar way with platinum and
suggests a second thio-keto substitution to somewhat enhance the *trans* influence of the ligand on the
ammonia loss.

1
2
3 The same lowest energy fragmentation routes by loss of NH₃ and HCl occur when *cis*-
4 [PtCl(NH₃)₂(L)]⁺ ions are assayed by IRMPD spectroscopy in both the explored fingerprint and
5 NH/OH stretching ranges, while the higher energy-demanding L elimination is not detected.
6
7

8
9
10 This evidence is in agreement with the notion that both multiple photon absorption and low-energy
11 CID are slow heating processes that promote fragmentation along the lowest energy channel [65, 66].
12

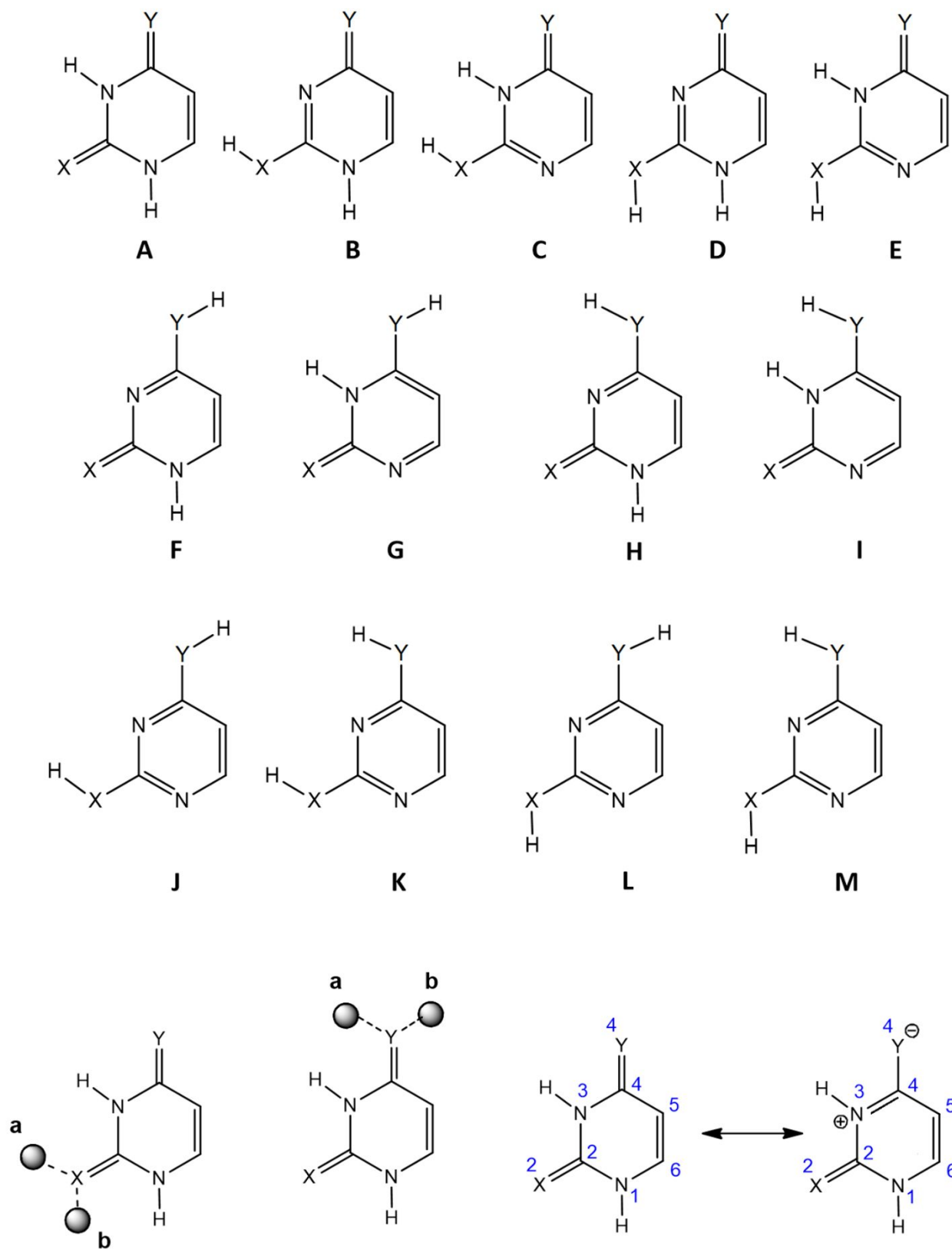
13 Exemplary mass spectra obtained when mass-selected *cis*-[PtCl(NH₃)₂(L)]⁺ are irradiated with the
14 CLIO FEL light tuned at 1810 (L=U), 1490 (2SU), 1280 (L=4SU) and 1285 (L=24dSU) cm⁻¹ are
15
16
17
18
19 illustrated in Figure S7-10, respectively.
20

21 **IRMPD Spectra.** The potential of IRMPD spectroscopy to elucidate structural features and to
22 distinguish isomers/conformers of a wide variety of (bio)molecular ions has been taken advantage of in
23 the present study [47, 67-69]. In the mid-IR range, the IRMPD spectra of *cis*-[PtCl(NH₃)₂(L)]⁺ (L=U,
24 2SU, 4SU, 24dSU) presented in Figure 2 exhibit distinct profiles, where prominent absorptions at high
25 wavenumber values highlight differences ascribable to the thio-keto substitution. While two strong,
26 poorly resolved bands at 1580 and 1615 cm⁻¹, a sharp peak at 1800 cm⁻¹ and two small absorptions at
27 1426 and 1480 cm⁻¹ are recorded for *cis*-[PtCl(NH₃)₂(U)]⁺, an intense broad peak centered at 1560 cm⁻¹
28
29
30
31
32
33
34
35
36
37
38
39
40
41
42
43
44
45
46
47
48
49
50
51
52
53
54
55
56
57
58
59
60
dominates the spectrum of *cis*-[PtCl(NH₃)₂(2SU)]⁺ with two shoulders on both red and blue sides at
1488 and 1619 cm⁻¹ and a very small absorption, likely due to a carbonyl stretch, at 1770 cm⁻¹. With
regard to *cis*-[PtCl(NH₃)₂(4SU)]⁺, two sharp strong peaks appear at 1609 and 1808 cm⁻¹, whereas the
IRMPD spectrum of *cis*-[PtCl(NH₃)₂(24dSU)]⁺ exhibits an intense broad feature, whose partial
resolution in bands centered at 1554 and 1586 cm⁻¹ has been attained at an attenuated laser pulse
energy of ca. 14 mJ/pulse. Below 1300 cm⁻¹, *cis*-[PtCl(NH₃)₂(4SU)]⁺ presents three sharp peaks at
1098, 1193 and 1279 cm⁻¹ which find a counterpart in: i) two small absorptions at 1209 and 1290 cm⁻¹
for *cis*-[PtCl(NH₃)₂(U)]⁺; ii) an envelope of bands between 1145 and 1240 cm⁻¹ and an intense and
broad one at 1297 cm⁻¹ for *cis*-[PtCl(NH₃)₂(2SU)]⁺; three weak bands at 1094, 1123-1163 and 1194
cm⁻¹ and an intense feature at 1280 cm⁻¹ for *cis*-[PtCl(NH₃)₂(24dSU)]⁺.

1
2
3 In the NH/OH stretching range, all IRMPD spectra are dominated by a strong band at 3462 (L=U),
4
5 3557 (L=2SU), 3445 (L=4SU) and 3452 (L= 24dSU) cm⁻¹, along with weaker bands at 3397 cm⁻¹ for
6
7 *cis*-[PtCl(NH₃)₂(2SU)]⁺, and at 3285, 3380 and 3431 cm⁻¹ for *cis*-[PtCl(NH₃)₂(24dSU)]⁺.
8
9

10 11 12 **Structural Characterization of the *cis*-[PtCl(NH₃)₂(L)]⁺ Complexes.**

13
14
15 **Computational Study.** The potential energy surface for the four *cis*-[PtCl(NH₃)₂(L)]⁺ (L=U, 2SU,
16
17 4SU, 24dSU) complexes, has been extensively explored in order to interpret their IRMPD spectra and
18
19 gain a structural characterization. To this end, 13 different tautomers of uracil and thiouracils have
20
21 been considered, whose optimized structures and corresponding relative free energies at 298 K (kJ
22
23 mol⁻¹) are given in Figures 3-6. Tables S1-S2 in the Supporting Information provide comprehensive
24
25 thermodynamic information on these and other identified structures deriving from canonical and
26
27 alternative forms, while the whole set of optimized geometries are reported in Figures S12-S15 in the
28
29 SI. In order to label the structures, the **T_Znm** nomenclature has been adopted, where **T** identifies the
30
31 tautomer considered, as shown in Scheme 1, **Z** is the binding atom (O, N or S), **n** being the atom
32
33 number, and **m** (m= a, b, c...) a letter which identifies the different conformers for a given
34
35 coordination scheme. To be noted, for the canonical form of the nucleobase (**A**), the letter **a** (**b**) was
36
37 systematically attributed to the complex in which the Pt atom is pointing towards (away from) the N3
38
39 center (Scheme 1).
40
41
42
43
44
45
46
47
48
49
50
51
52
53
54
55
56
57
58
59
60



Scheme 1. Nomenclature adopted and zwitterionic effect for U (X=Y=O), 2SU (X=S, Y=O), 4SU (X=O, Y=S) and 24dSU (X=Y=S).

1
2
3
4
5
6 If one first considers the uracil complexes, *cis*-[PtCl(NH₃)₂U]⁺, one may note that the most stable
7
8 form, **A_O4a**, is characterized by *cis*-[PtCl(NH₃)₂]⁺ binding with the O4 keto center of uracil, the
9
10 metal leaning towards N3 (Figure 3). The structure **A_O4b**, associated with the alternate
11
12 orientation, is found ~12 kJ/mol higher in energy, probably due to the loss of the hydrogen bond
13
14 between the chlorine atom and the NH group. Examination of Figure 3 also shows that binding with
15
16 O2 results in less stable forms. Concerning the canonical forms of uracil, this behavior has already
17
18 been reported for complexation by alkali cations [33, 58, 60], Cu⁺ and Cu²⁺ ions [27, 70], as well as
19
20 Ca²⁺ and Pb²⁺ [29, 30], and may be attributed to the so-called “zwitterionic effect” introduced some
21
22 years ago by Lamsabhi et al. [11] In this study, it was shown through the analysis of the charge
23
24 distribution of uracil and thiouracils that the contribution of zwitterionic resonance structures is
25
26 important in this kind of interaction. This effect results in an increased negative charge on the
27
28 heteroatom at position 4 (Y) with respect to the one attached to position 2 (X), and therefore in an
29
30 increase of its intrinsic basicity towards the approaching Lewis acid. We also considered the
31
32 possible coordination of the Pt center with enol groups (see for example **C_O2** or **F_O4** forms) of
33
34 tautomeric forms. Such interactions result in significantly less stable structures, as attested by the
35
36 computed relative free energies. On the other hand, several structures, all characterized by the
37
38 occurrence of intramolecular hydrogen bonds involving the amino or chlorido ligands of the *cis*-
39
40 [PtCl(NH₃)₂]⁺ moiety and an electronegative atom or NH group of the nucleobase, appear
41
42 particularly stable. This is notably the case of the tautomeric forms **H_O2c** and **H_N3**, the latter
43
44 lying at the same energy level as **A_O4a**. For Ca²⁺ and Cu²⁺ ions, theoretical studies have
45
46 demonstrated that complexes involving tautomeric forms of uracil are much more stable than those
47
48 involving canonical forms, the associated proton shift allowing bidentate interactions with O2 and
49
50 N3 centers. [27, 30]
51
52
53
54
55
56
57
58
59
60

1
2
3 Examination of the structures optimized with canonical 2-thiouracil (Figure 4) shows that the
4 preferred coordination site also depends on the nature of the heteroatom involved in the interaction.
5
6 Our results confirm that the Pt center displays a stronger affinity for sulfur than for oxygen,
7
8 probably due to the greater polarizability of sulfur. This evidence has already been reported for
9
10 “soft” ions like Cu^+ [70], whereas the association of “hard” alkali cations or Cu^{2+} ions with the
11
12 oxygen atom is systematically favored when the systems present both types of basic centers, that is,
13
14 a keto and a thioketo group. [27, 33, 60] Unlike previous evidence on Pb^{2+} ions [29], in presence of
15
16 the *cis*- $[\text{PtCl}(\text{NH}_3)_2]^+$ species, the enhanced affinity for sulfur outcompetes the zwitterionic effect in
17
18 the case of 2-thiouracil, leading to **A_S2** forms significantly more stable than **A_O4** structure, the
19
20 latter geometry being now located 36.9 kJ/mol above the global minimum (**A_S2b**, Figure 4). We
21
22 also optimized numerous structures involving tautomeric forms of 2SU. One form, namely **H_S2c**
23
24 is found particularly stable, but remains slightly above the canonical **A_S2b** form (+3.7 kJ/mol).
25
26 Within **H_S2c**, the coordination remains monodentate satisfying the square planar coordination of
27
28 platinum(II), whereas bidentate interactions with tautomeric forms were reported as the most stable
29
30 structures for Cu^{2+} and Ca^{2+} ions. [27, 30]
31
32
33
34
35
36

37 In the case of 4-thiouracil, the zwitterionic effect and the bias for platinum binding to sulfur concur
38
39 in favoring coordination to S4 (**A_S4a**, Figure 5), the relative free energy difference with the
40
41 **A_O2b** isomer reaching now ~60 kJ/mol. The binding scheme observed in presence of cisplatin
42
43 therefore differs from the one reported for alkali cations [33, 60], as well as for Cu^{2+} and Ca^{2+} ions
44
45 [27, 30] (preferred interaction with O2). Unlike uracil and 2-thiouracil, competitive tautomeric
46
47 forms were not identified, the most stable, **E_S4a**, being 32.2 kJ/mol above the global minimum
48
49 **A_S4a**.
50
51
52

53 Finally, in presence of 2,4-dithiouracil which, like uracil, has equal X and Y basic centers, the most
54
55 favorable coordination scheme (**A_S4a**, Figure 6) is driven only by the zwitterionic effect, with
56
57 relative free energies comparable to those computed for uracil (Figure 3) , in agreement with
58
59
60

1
2
3 previous evidence [27-30, 58-60]. Noteworthy, a very stable complex involving a tautomeric form,
4 **H_S2c**, is located on the potential energy surface, which is similar to the stable tautomeric form
5
6 obtained with 2-thiouracil (*vide supra*).
7
8

9
10 **IRMPD Spectra of *cis*-[PtCl(NH₃)₂(L)]⁺ Complexes.** According to the computational analysis
11
12 that points to a coordination scheme governed by the distinct contribution of a zwitterionic effect
13
14 and the strong cisPt affinity for sulfur, different types of structures are likely to be present in the
15
16 sampled ion population, depending on the number of sulfur atoms. This notion is consistent with the
17
18 experimental findings by IRMPD spectroscopy (Figure 2), both in the fingerprint and the X-H
19
20 stretch regions.
21
22

23
24 ***cis*-[PtCl(NH₃)₂(U)]⁺ complex.** For this system, several structures are close in energy, two of them
25
26 being degenerate (**A_O4a** and **H_N3**), thus suggesting that a mixture of tautomers might contribute
27
28 to the sampled ion population. As a consequence, IRMPD spectroscopy can be particularly helpful
29
30 to decipher the presence of multiple forms. In the fingerprint region, the IRMPD spectrum recorded
31
32 for the *cis*-[PtCl(NH₃)₂(U)]⁺ complex has been compared with the DFT-computed vibrational
33
34 spectra of low-lying structures (Figure 7). A very good agreement emerges between the
35
36 experimental trace and the vibrational spectra computed for the O4-coordinated complexes (**A_O4a**
37
38 and **A_O4b**; Figure 7c-d). The positions and intensities of the major IR active modes of these two
39
40 forms are summarized in Table S3 of the Supporting Information. In particular, the IRMPD band
41
42 detected at 1209 cm⁻¹ can be interpreted as a combination of C-H and N1-H bending modes of
43
44 uracil. The IRMPD signal detected at 1290 cm⁻¹ can be assigned to the NH₃' umbrella bending
45
46 mode (by convention the NH₃' group corresponds to the ammonia group in the *trans* position with
47
48 respect to the chlorine atom). The weak bands measured at 1426 and 1480 cm⁻¹ correspond to the
49
50 N1H bending mode and the stretches of C4C5 and N1C6 bonds, respectively. The pronounced
51
52 feature at 1580 cm⁻¹ is ascribed to the C4O4 stretching mode, therefore significantly red-shifted as
53
54 compared to an unperturbed C=O stretch, due to the interaction with Pt. As an additional argument,
55
56
57
58
59
60

1
2
3 the C2=O2 stretch computed at 1817-1819 wavenumbers for both forms, **A_O4a** and **A_O4b**, well
4 reproduces the experimental band at 1800 cm⁻¹. The most intense signal, detected at 1615 cm⁻¹, may
5 be assigned to the C5C6 stretching mode. The **A_O2b** structure (Figure 7b) cannot be excluded on
6 the basis of the spectroscopic features, although this structure does not correctly reproduce the
7 experimental trace recorded between 1560 and 1620 cm⁻¹. Contrarily, the **H_N3** form, even if
8 degenerate with the global minimum, can be reasonably discarded (Figure 7a). Finally, in the X-H
9 stretch region, only one particularly intense band was detected at 3452 cm⁻¹. The signal is well
10 reproduced by the N1-H stretching mode of both **A_O4a** and **A_O4b**. Vibrational modes associated
11 to (strongly) hydrogen-bonded networks are barely observed in the experimental spectrum,
12 including the intense N3-H stretch predicted for **A_O4a** at 3183 cm⁻¹, and the weaker asymmetric
13 NH₂ stretches of NH₃ and NH₃' in the 3370-3394 cm⁻¹ and 3345-3392 cm⁻¹ ranges for **A_O4a** and
14 **A_O4b**, respectively. A similar behavior where H-bond interactions are not faithfully revealed has
15 been already described as "IRMPD transparency" and reported for several (bio)molecular systems
16 [71-73]. To summarize, comparison between IRMPD data and DFT calculations demonstrate that
17 the *cis*-[Pt(NH₃)₂Cl(U)]⁺ complex is mainly characterized by coordination the *cis*Pt moiety with O4
18 of the canonical form of uracil.

19
20
21
22
23
24
25
26
27
28
29
30
31
32
33
34
35
36
37
38
39
40
41 ***cis*-[PtCl(NH₃)₂(2SU)]⁺ Complex.** As illustrated in Figure 2, the experimental IRMPD spectrum of
42 *cis*-[PtCl(NH₃)₂(2SU)]⁺ differs significantly from the one of the uracil complex. The comparison
43 shown in Figure 8 indicates a very good agreement with the vibrational spectra computed for the
44 global minimum, **A_S2b** and its rotamer **A_S2a**. Notably, both structures correctly reproduce the
45 shape and the intensity of the experimental profile recorded between 1450 cm⁻¹ and 1650 cm⁻¹, due
46 to three bands attributed to N1C2 bond stretch, NH bending and NH₂ scissoring modes of both NH₃
47 and NH₃' groups, and to C5C6 bond stretch (Table S4). Other signals are also well reproduced. The
48 band at 1770 cm⁻¹ is attributed to the stretch of the C4=O4 carbonyl group computed at 1790 cm⁻¹.
49 The broad band at 1297 cm⁻¹ corresponds to the umbrella modes of NH₃' and NH₃, whereas series
50
51
52
53
54
55
56
57
58
59
60

1
2
3 of unresolved features between 1145 and 1240 cm^{-1} may be ascribed to CH bending modes coupled
4 with C2S2 stretch. In the X-H stretching region, the IRMPD spectrum is also different from that
5 recorded with uracil as it exhibits two peaks, detected at 3405 and 3569 cm^{-1} . Remarkably, the latter
6 signal cannot be interpreted by vibrations of the S2-coordinated tautomer A, but rather suggests the
7 presence a certain fraction of **H_S2c**, tautomer of **A_S2b**, which lies only 3.7 kJ/mol above the
8 global minimum and presents a free O4H stretch calculated at 3578 cm^{-1} . Its vibrational spectrum
9 also matches most of the bands observed in the fingerprint region, albeit with less overall
10 agreement. Consequently, IRMPD data for 2SU seem to point to a mixture of tautomeric forms
11 sharing the same coordination scheme (monodentate interaction with S2). Accordingly, formation
12 of tautomeric forms have also been reported recently for protonated 2SU [15].

13
14
15
16
17
18
19
20
21
22
23
24
25
26 ***cis*-[PtCl(NH₃)₂(4SU)]⁺ Complex.** Again, the situation changes drastically when considering 4-
27 thiouracil, thus allowing the two isomers of thiouracil complexes to be easily distinguished by
28 IRMPD spectroscopy. As shown in Figure 9e, the experimental IRMPD spectrum in the fingerprint
29 region exhibits five sharp signals with an unperturbed carbonyl group at 1808 cm^{-1} , indicating a
30 structure where the C2=O2 group does not interact with the metal. Consistently, the spectra
31 computed for the **A_S4a** and **A_S4b** rotamers (Figure 9c-d) perfectly reproduce all the
32 experimental bands. By order of increasing wavenumber, the three peaks at 1098, 1279, and 1609
33 cm^{-1} can be ascribed to C4S4 and C2N3 stretches, NH₃ and NH₃' umbrella, and C5C6 stretch mode
34 (Table S5). Formation of an O2-coordinated complex, lacking the carbonyl stretch, is unlikely
35 because of a poorer agreement (Figure 9b), as expected from a structure which is already 60 kJ/mol
36 higher in energy (*vide supra*). Finally, the tautomeric form **E_S4a** can also be discarded as it cannot
37 account for any of the two absorptions observed at 1808 and 1098 cm^{-1} . In the X-H stretch region,
38 this form should give a strong band at about 3600 cm^{-1} , due to the free O2H stretch, which is
39 missing in the IRMPD spectrum, and cannot account for the only signal observed experimentally at
40 3445 cm^{-1} . Such a strong single peak, computed for both **A_S4a** and **A_S4b**, is due to the free N1H
41
42
43
44
45
46
47
48
49
50
51
52
53
54
55
56
57
58
59
60

1
2
3 stretch. As a consequence, our data suggest that a single type of structure is generated in presence of
4
5 4-thiouracil, characterized by the complexation of the cisPt moiety onto the sulfur atom of the
6
7 canonical form. This was quite expected based on the computational survey where additive effects
8
9 predict a favored attack at S4.

10
11 ***cis*-[PtCl(NH₃)₂(24dSU)]⁺ Complex.** Figure 10f shows the experimental IRMPD spectrum
12
13 compared with the IR spectra computed for low-lying S4- and S2-coordinated complexes (Figure
14
15 10a-e). Notably, the best agreement is obtained with the S4 forms, well accounting for the feature
16
17 recorded above 1500 cm⁻¹, which can be interpreted as the combination of C2S2 and C5C6
18
19 stretches, computed at 1556 and 1591 cm⁻¹, respectively (Table S6). The three experimental signals
20
21 detected below 1400 cm⁻¹ are also well reproduced by both **A_S4a** and **A_S4b**, although this
22
23 finding is also true for the other structures. Remarkably, **H_S2c** and **A_S2b** isomers are the only
24
25 ones that reproduce the weak experimental band at 1445 cm⁻¹, suggesting that a minor contribution
26
27 of these species may likely occur. This is a reasonable assumption as a previous IRMPD study has
28
29 shown that sodium cationization promotes the stabilization of a minor tautomer of 24dSU [32].
30
31
32
33

34
35 Examination of the IRMPD spectrum recorded in the OPO range shows that the three experimental
36
37 signals detected at 3285, 3380 and 3431 cm⁻¹ are well reproduced by the vibrational spectra of
38
39 **A_S4a** and **A_S4b**, corresponding to the symmetric and asymmetric stretches of the ammonia
40
41 ligands, and free N1H stretch, respectively. The N3H stretch computed at 3400 cm⁻¹ in the case of
42
43 **A_S4b**, is red-shifted at 3224 cm⁻¹ for **A_S4a** due to the hydrogen bond established with the
44
45 chlorine atom. According to previous discussion, this particular signal is barely observed
46
47 experimentally. Finally, the weak shoulder detected at 3446 cm⁻¹ is reproduced neither by the
48
49 couple **A_S4a/A_S4b**, nor by the tautomeric form **H_S2c**, thus suggesting that some amount of an
50
51 additional structure could be present. This form might correspond to a S2-coordinated complex, as
52
53 the N1H stretch computed at 3451 cm⁻¹ for **A_S2a** satisfyingly matches with the experimental band
54
55
56
57
58
59
60

(3446 cm⁻¹). In summary, the interaction of cisPt with 24dSU likely originates a mixture of different forms, the canonical S4-coordinated complexes being largely the most populated.

Conclusions

The interaction between the antitumor drug cisplatin and four (thio)uracils in aqueous methanol solution yields monofunctional primary complexes *cis*-[PtCl(NH₃)₂(L)]⁺, that were extracted by ESI and delivered to the gas phase as isolated species to be characterized by IR spectroscopy in the complementary hydrogen-stretching and fingerprint ranges. The prevailing dissociation channel observed upon both CID and IRMPD assay, involving loss of NH₃, is consistent with the dominant process previously reported for similar cisplatin adducts [37,38,40-42].

The experimentally accessed structures have been identified by comparison with the linear IR spectra of candidate structures generated by quantum chemical calculations.

The ground-state structures of *cis*-[PtCl(NH₃)₂(L)]⁺ complexes have shown sulfur as the preferred complexation site. The most favored binding of platinum is directed to the O4(S4) atoms of the canonical forms of U, 4SU and 24dSU, and to the S2 atom of 2SU. However, the present results suggest that, while *cis*-[PtCl(NH₃)₂(L)]⁺ (L=U, 4SU) are represented by a single canonical structure, platinum(II) cationization stabilizes also minor, non-canonical tautomers for L= 2SU and 24dSU. Therefore, although to a much more limited extent relative to protonation, also the *cis*-[PtCl(NH₃)₂]⁺ subunit of cisplatin shows an augmented prospect of nucleic acid strand disorder.

ASSOCIATED CONTENT

Supporting Information

The Supporting Information is available free of charge at <https://pubs.acs.org/doi/...>

Figures S1-S14.

1
2
3 CID mass spectra (Figures S1-S4). Breakdown curves (Figures S4-S6). ESI mass spectra after
4 irradiation with CLIO FEL light (Figures S7-S10). Optimized geometries and relative free energy
5 values (Figures S11-S14).

6
7
8 Tables S1-S6.

9
10 Thermodynamic data (Tables S1-S2). Experimental and computed IR bands (Tables S3-S6).

11 12 13 **AUTHOR INFORMATION**

14 15 16 **Corresponding Authors:**

17
18 *to Maria Elisa Crestoni; email: mariaelisa.crestoni@uniroma1.it

19
20 *to Jean-Yves Salpin; email: jeanyves.salpin@univ-evry.fr

21 22 23 **ORCID**

24 Davide Corinti: [0000-0001-8064-3492](https://orcid.org/0000-0001-8064-3492)

25 Maria Elisa Crestoni: [0000-0002-0991-5034](https://orcid.org/0000-0002-0991-5034)

26 Barbara Chiavarino: [0000-0002-1585-7061](https://orcid.org/0000-0002-1585-7061)

27 Simonetta Fornarini: [0000-0002-6312-5738](https://orcid.org/0000-0002-6312-5738)

28 Debora Scuderi: [0000-0003-3931-8481](https://orcid.org/0000-0003-3931-8481)

29 Jean-Yves Salpin: [0000-0003-0979-1251](https://orcid.org/0000-0003-0979-1251)

30 31 32 33 34 35 36 **Notes**

37 The authors declare no competing financial interest.

38 39 40 41 42 **Acknowledgements**

43 We are grateful to Jean-Michel Ortega, Philippe Maitre, V. Steinmetz and the CLIO team. This
44 work was supported by the Italian Ministry for Education, University and Research – Dipartimenti
45 di Eccellenza - L. 232/2016 and by the project CALIPSO plus under the Grant Agreement No.
46 730872 from the EU Framework Program for Research and Innovations HORIZON 2020. Financial
47 Support from the National FT-ICR network (No. FR3624 CNRS) for conducting the research is
48 gratefully acknowledged. J-Y.S. is grateful to the computational centre of the Universidad
49 Autónoma de Madrid for computing facilities.

50 51 52 53 54 55 **References**

56 [1] Neidle, S.: Principles of Nucleic Acid Structure, Academic Press, 2008.

- 1
2
3 [2] Saenger, W., Suck, D.: The Relationship between Hydrogen Bonding and Base Stacking in Crystalline 4-
4 Thiouridine Derivatives. *Eur. J. Biochem.* 32, 473–478 (1973). <https://doi.org/10.1111/j.1432-1033.1973.tb02630.x>
5
6
7
8 [3] Scheit, K.H., Gaertner, E.: Properties Of Polynucleotides Containing Uridine And 4-Thiouridine (S4U).
9 *Biochim. Biophys. Acta - Nucleic Acids Protein Synth.* 182, 10–16 (1969). [https://doi.org/10.1016/0005-2787\(69\)90514-0](https://doi.org/10.1016/0005-2787(69)90514-0)
10
11
12 [4] Gottschalk, E.M., Kopp, E., Lezius, A.G.: A Synthetic DNA with Unusual Base-Pairing. *Eur. J.*
13 *Biochem.* 24, 168–182 (1971). <https://doi.org/10.1111/j.1432-1033.1971.tb19668.x>
14
15 [5] Beak, P.: Energies and alkylations of tautomeric heterocyclic compounds: old problems - new answers.
16 *Acc. Chem. Res.* 10, 186–192 (1977). <https://doi.org/10.1021/ar50113a006>
17
18 [6] Rostkowska, H., Barski, A., Szczepaniak, K., Szczesniak, M., Person, W.B.: The tautomeric equilibria of
19 thioanalogues of nucleic acids: spectroscopic studies of 2-thiouracils in the vapour phase and in low
20 temperature matrices. *J. Mol. Struct.* 176, 137–147 (1988). [https://doi.org/10.1016/0022-2860\(88\)80237-0](https://doi.org/10.1016/0022-2860(88)80237-0)
21
22 [7] Katritzky, A.R., Baykut, G., Rachwal, S., Szafran, M., Caster, K.C., Eyler, J.: The tautomeric equilibria
23 of thio analogues of nucleic acid bases. Part 1. 2-Thiouracil: background, preparation of model compounds,
24 and gas-phase proton affinities. *J. Chem. Soc. Perkin Trans. 2.* 1499 (1989).
25 <https://doi.org/10.1039/p29890001499>
26
27 [8] Rostkowska, H., Szczepaniak, K., Nowak, M.J., Leszczynski, J., Kubulat, K., Person, W.B.: Studies of
28 Thiouracils .2. Tautomerism and Infrared-Spectra of Thiouracils - Matrix-Isolation and Abinitio Studies. *J.*
29 *Am. Chem. Soc.* 112, 2147–2160 (1990).
30
31 [9] Les, A., Adamowicz, L.: Tautomerism of 2- and 4-thiouracil. Ab initio theoretical study. *J. Am. Chem.*
32 *Soc.* 112, 1504–1509 (1990). <https://doi.org/10.1021/ja00160a032>
33
34 [10] Yekeler, H.: Ab initio study on tautomerism of 2-thiouracil in the gas phase and in solution. *J. Comput.*
35 *Aided. Mol. Des.* 14, 243–250 (2000). <https://doi.org/10.1023/a:1008132202838>
36
37 [11] Lamsabhi, M., Alcamí, M., Mó, O., Bouab, W., Esseffar, M., Abboud, J.L.-M., Yáñez, M.: Are the
38 Thiouracils Sulfur Bases in the Gas-phase? *J. Phys. Chem. A.* 104, 5122–5130 (2000).
39 <https://doi.org/10.1021/jp000071k>
40
41 [12] Kryachko, E., Nguyen, M.T., Zeegers-Huyskens, T.: Thiouracils: Acidity, basicity, and interaction with
42 water. *J. Phys. Chem. A.* 105, 3379–3387 (2001)
43
44 [13] Marino, T., Russo, N., Sicilia, E., Toscano, M.: Tautomeric equilibria of 2- and 4-thiouracil in gas phase
45 and in solvent: A density functional study. *Int. J. Quantum Chem.* 82, 44–52 (2001).
46 [https://doi.org/10.1002/1097-461X\(2001\)82:1<44::AID-QUA1020>3.0.CO;2-6](https://doi.org/10.1002/1097-461X(2001)82:1<44::AID-QUA1020>3.0.CO;2-6)
47
48 [14] Lamsabhi, A.M., Mó, O., Gutiérrez-Oliva, S., Pérez, P., Toro-Labbé, A., Yáñez, M.: The mechanism of
49 double proton transfer in dimers of uracil and 2-thiouracil-The reaction force perspective. *J. Comput. Chem.*
50 30, 389–398 (2009). <https://doi.org/10.1002/jcc.21064>
51
52
53
54
55
56
57
58
59
60

- 1
2
3 [15] Nei, Y. -w., Akinyemi, T.E., Steill, J.D., Oomens, J., Rodgers, M.T.: Infrared multiple photon
4 dissociation action spectroscopy of protonated uracil and thiouracils: Effects of thioketo-substitution on gas-
5 phase conformation. *Int. J. Mass Spectrom.* 297, 139–151 (2010). <https://doi.org/10.1016/j.ijms.2010.08.005>
6
7 [16] Colasurdo, D.D., Pila, M.N., Iglesias, D.A., Laurella, S.L., Ruiz, D.L.: Tautomerism of uracil and
8 related compounds: A mass spectrometry study. *Eur. J. Mass Spectrom.* 24, 214–224 (2018).
9 <https://doi.org/10.1177/1469066717712461>
10
11 [17] Astwood, E.B., Bissell, A., Hughes, A.M.: Further Studies On The Chemical Nature Of Compounds
12 Which Inhibit The Function Of The Thyroid Gland 1 1. *Endocrinology.* 37, 456–481 (1945).
13 <https://doi.org/10.1210/endo-37-6-456>
14
15 [18] Hercbergs, A.A., Goyal, L.K., Suh, J.H., Lee, S., Reddy, C.A., Cohen, B.H., Stevens, G.H., Reddy,
16 S.K., Peereboom, D.M., Elson, P.J., Gupta, M.K., Barnett, G.H.: Propylthiouracil-induced chemical
17 hypothyroidism with high-dose tamoxifen prolongs survival in recurrent high grade glioma: a phase I/II
18 study. *Anticancer Res.* 23, 617–26 (2003)
19
20 [19] Jeener, R., Rosseels, J.: Incorporation Of 2-Thiouracil-S-35 In The Ribose Nucleic Acid Of Tobacco
21 Mosaic Virus. *Biochim. Biophys. Acta.* 11, 438 (1953). [https://doi.org/10.1016/0006-3002\(53\)90063-8](https://doi.org/10.1016/0006-3002(53)90063-8)
22
23 [20] Abdel-Rahman, A.A.H., Abdel-Megied, A.E.S., Goda, A.E.S., Zeid, I.F., El Ashry, E.S.H.: Synthesis
24 and anti-HBV activity of thiouracils linked via S and N-1 to the 5-position of methyl beta-D-ribofuranoside.
25 *Nucleosides Nucleotides & Nucleic Acids.* 22, 2027–2038 (2003). <https://doi.org/10.1081/ncn-120026404>
26
27 [21] Theodossiou, C., Schwarzenberger, P.: Propylthiouracil Reduces Xenograft Tumor Growth in an
28 Athymic Nude Mouse Prostate Cancer Model. *Am. J. Med. Sci.* 319, 96 (2000).
29 <https://doi.org/10.1097/00000441-200002000-00005>
30
31 [22] Macchia, M., Barontini, S., Bertini, S., Di Bussolo, V., Fogli, S., Giovannetti, E., Grossi, E., Minutolo,
32 F., Danesi, R.: Design, Synthesis, and Characterization of the Antitumor Activity of Novel Ceramide
33 Analogues. *J. Med. Chem.* 44, 3994–4000 (2001). <https://doi.org/10.1021/jm010947r>
34
35 [23] Gredilla, R., Barja, G., López-Torres, M.: Thyroid hormone-induced oxidative damage on lipids,
36 glutathione and DNA in the mouse heart. *Free Radic. Res.* 35, 417–425 (2001).
37 <https://doi.org/10.1080/10715760100300931>
38
39 [24] Ortega-Carvalho, T.M., Hashimoto, K., Pazos-Moura, C.C., Geenen, D., Cohen, R., Lang, R.M.,
40 Wondisford, F.E.: Thyroid hormone resistance in the heart: Role of the thyroid hormone receptor beta
41 isoform. *Endocrinology.* 145, 1625–1633 (2004). <https://doi.org/10.1210/en.2003-1031>
42
43 [25] Soliman, E.M., Ahmed, S.A.: Selective separation of silver(I) and mercury(II) ions in natural water
44 samples using alumina modified thiouracil derivatives as new solid phase extractors. *Int. J. Environ. Anal.*
45 *Chem.* 89, 389–406 (2009). <https://doi.org/10.1080/03067310902719142>
46
47 [26] Zhou, N., Chen, H., Li, J., Chen, L.: Highly sensitive and selective voltammetric detection of
48 mercury(II) using an ITO electrode modified with 5-methyl-2-thiouracil, graphene oxide and gold
49 nanoparticles. *Microchim. Acta.* 180, 493–499 (2013). <https://doi.org/10.1007/s00604-013-0956-0>
50
51
52
53
54
55
56
57
58
59
60

- [27] Lamsabhi, A.M., Alcamí, M., Mó, O., Yáñez, M., Tortajada, J.: Association of Cu²⁺ with Uracil and Its Thio Derivatives: A Theoretical Study. *ChemPhysChem*. 5, 1871–1878 (2004). <https://doi.org/10.1002/cphc.200400208>
- [28] Lamsabhi, A.M., Alcamí, M., Mó, O., Yáñez, M., Tortajada, J.: Gas-Phase Deprotonation of Uracil–Cu²⁺ and Thiouracil–Cu²⁺ Complexes. *J. Phys. Chem. A*. 110, 1943–1950 (2006). <https://doi.org/10.1021/jp055163u>
- [29] Salpin, J.-Y., Guillaumont, S., Tortajada, J., Lamsabhi, M.: Gas-phase interactions between lead(II) ions and thiouracil nucleobases: A combined experimental and theoretical study. *J. Am. Soc. Mass Spectrom.* 20, 359–369 (2009). <https://doi.org/10.1016/j.jasms.2008.10.015>
- [30] Trujillo, C., Lamsabhi, A.M., Mó, O., Yáñez, M., Salpin, J.-Y.: Interaction of Ca²⁺ with uracil and its thio derivatives in the gas phase. *Org. Biomol. Chem.* 6, 3695 (2008). <https://doi.org/10.1039/b810418b>
- [31] Corral, I., Trujillo, C., Salpin, J.Y., Yáñez, M.: *Kinetics and Dynamics: from Nano- to Bio-Scale*. Springer (2010)
- [32] Salpin, J.-Y., Guillaumont, S., Tortajada, J., MacAleese, L., Lemaire, J., Maitre, P.: Infrared Spectra of Protonated Uracil, Thymine and Cytosine. *ChemPhysChem*. 8, 2235–2244 (2007). <https://doi.org/10.1002/cphc.200700284>
- [33] Nei, Y.-w., Akinyemi, T.E., Kaczan, C.M., Steill, J.D., Berden, G., Oomens, J., Rodgers, M.T.: Infrared multiple photon dissociation action spectroscopy of sodiated uracil and thiouracils: Effects of thioketo-substitution on gas-phase conformation. *Int. J. Mass Spectrom.* 308, 191–202 (2011). <https://doi.org/10.1016/j.ijms.2011.06.019>
- [34] Akinyemi, T.E., Wu, R.R., Nei, Y.-W., Cunningham, N.A., Roy, H.A., Steill, J.D., Berden, G., Oomens, J., Rodgers, M.T.: Influence of Transition Metal Cationization versus Sodium Cationization and Protonation on the Gas-Phase Tautomeric Conformations and Stability of Uracil: Application to [Ura+Cu]⁺ and [Ura+Ag]⁺. *J. Am. Soc. Mass Spectrom.* 28, 2438–2453 (2017). <https://doi.org/10.1007/s13361-017-1771-3>
- [35] Hamlow, L.A., Zhu, Y., Devereaux, Z.J., Cunningham, N.A., Berden, G., Oomens, J., Rodgers, M.T.: Modified Quadrupole Ion Trap Mass Spectrometer for Infrared Ion Spectroscopy: Application to Protonated Thiated Uridines. *J. Am. Soc. Mass Spectrom.* 29, 2125–2137 (2018). <https://doi.org/10.1007/s13361-018-2047-2>
- [36] De Petris, A., Ciavardini, A., Coletti, C., Re, N., Chiavarino, B., Crestoni, M.E., Fornarini, S.: Vibrational signatures of the naked aqua complexes from platinum(II) anticancer drugs. *J. Phys. Chem. Lett.* 4, 3631–3635 (2013). <https://doi.org/10.1021/jz401959s>
- [37] Corinti, D., De Petris, A., Coletti, C., Re, N., Chiavarino, B., Crestoni, M.E., Fornarini, S.: Cisplatin Primary Complex with l-Histidine Target Revealed by IR Multiple Photon Dissociation (IRMPD) Spectroscopy. *ChemPhysChem*. 18, 318–325 (2017). <https://doi.org/10.1002/cphc.201601172>
- [38] Paciotti, R., Corinti, D., De Petris, A., Ciavardini, A., Piccirillo, S., Coletti, C., Re, N., Maitre, P., Bellina, B., Barran, P., Chiavarino, B., Elisa Crestoni, M., Fornarini, S.: Cisplatin and transplatin interaction

- with methionine: bonding motifs assayed by vibrational spectroscopy in the isolated ionic complexes. *Phys. Chem. Chem. Phys.* 19, 26697–26707 (2017). <https://doi.org/10.1039/C7CP05203K>
- [39] He, C.C., Kimutai, B., Bao, X., Hamlow, L., Zhu, Y., Strobehn, S.F., Gao, J., Berden, G., Oomens, J., Chow, C.S., Rodgers, M.T.: Evaluation of Hybrid Theoretical Approaches for Structural Determination of a Glycine-Linked Cisplatin Derivative via Infrared Multiple Photon Dissociation (IRMPD) Action Spectroscopy. *J. Phys. Chem. A.* 119, 10980–10987 (2015). <https://doi.org/10.1021/acs.jpca.5b08181>
- [40] Chiavarino, B., Crestoni, M.E., Fornarini, S., Scuderi, D., Salpin, J.-Y.: Interaction of Cisplatin with Adenine and Guanine: A Combined IRMPD, MS/MS, and Theoretical Study. *J. Am. Chem. Soc.* 135, 1445–1455 (2013). <https://doi.org/10.1021/ja309857d>
- [41] Chiavarino, B., Crestoni, M.E., Fornarini, S., Scuderi, D., Salpin, J.-Y.: Interaction of Cisplatin with 5'-dGMP: A Combined IRMPD and Theoretical Study. *Inorg. Chem.* 54, 3513–3522 (2015). <https://doi.org/10.1021/acs.inorgchem.5b00070>
- [42] Chiavarino, B., Crestoni, M.E., Fornarini, S., Scuderi, D., Salpin, J.-Y.: Undervalued N3 Coordination Revealed in the Cisplatin Complex with 2'-Deoxyadenosine-5'-monophosphate by a Combined IRMPD and Theoretical Study. *Inorg. Chem.* 56, 8793–8801 (2017). <https://doi.org/10.1021/acs.inorgchem.7b00570>
- [43] Alessio, E. *Bioinorganic Medicinal Chemistry*, Wiley-VCH Verlag GmbH, Weinheim (2011)
- [44] Anderson, S.G., Blades, A.T., Klassen, J., Kebarle, P.: Determination of ion-ligand bond energies and ion fragmentation energies of electrospray-produced ions by collision-induced dissociation threshold measurements. *Int. J. Mass Spectrom. Ion Process.* 141, 217–228 (1995). [https://doi.org/10.1016/0168-1176\(94\)04110-S](https://doi.org/10.1016/0168-1176(94)04110-S)
- [45] Sinha, R.K., Maître, P., Piccirillo, S., Chiavarino, B., Crestoni, M.E., Fornarini, S.: Cysteine radical cation: A distonic structure probed by gas phase IR spectroscopy. *Phys. Chem. Chem. Phys.* 12, 9794 (2010). <https://doi.org/10.1039/c003576a>
- [46] Chiavarino, B., Crestoni, M.E., Fornarini, S., Taioli, S., Mancini, I., Tosi, P.: Infrared spectroscopy of copper-resveratrol complexes: A joint experimental and theoretical study. *J. Chem. Phys.* 137, 024307 (2012). <https://doi.org/10.1063/1.4732583>
- [47] Corinti, D., Crestoni, M.E., Fornarini, S., Pieper, M., Niehaus, K., Giampà, M.: An integrated approach to study novel properties of a MALDI matrix (4-maleicanhydridoproton sponge) for MS imaging analyses. *Anal. Bioanal. Chem.* 411, 953–964 (2019). <https://doi.org/10.1007/s00216-018-1531-7>
- [48] Glotin, F., Ortega, J., Prazeres, R., Rippon, C.: Activities of the CLIO infrared facility. *Nucl. Instruments Methods Phys. Res. Sect. B Beam Interact. with Mater. Atoms.* 144, 8–17 (1998). [https://doi.org/10.1016/S0168-583X\(98\)00293-6](https://doi.org/10.1016/S0168-583X(98)00293-6)
- [49] Lemaire, J., Boissel, P., Heninger, M., Mauclaire, G., Bellec, G., Mestdagh, H., Simon, A., Caer, S. Le, Ortega, J.M., Glotin, F., Maitre, P.: Gas Phase Infrared Spectroscopy of Selectively Prepared Ions. *Phys. Rev. Lett.* 89, 273002 (2002). <https://doi.org/10.1103/PhysRevLett.89.273002>

- [50] Bakker, J.M., Besson, T., Lemaire, J., Scuderi, D., Maître, P.: Gas-Phase Structure of a π -Allyl-Palladium Complex: Efficient Infrared Spectroscopy in a 7 T Fourier Transform Mass Spectrometer. *J. Phys. Chem. A* 111, 13415–13424 (2007). <https://doi.org/10.1021/jp074935e>
- [51] Prell, J.S., O'Brien, J.T., Williams, E.R.: IRPD spectroscopy and ensemble measurements: Effects of different data acquisition and analysis methods. *J. Am. Soc. Mass Spectrom.* 21, 800–809 (2010). <https://doi.org/10.1016/j.jasms.2010.01.010>
- [52] Lee, C., Yang, W., Parr, R.G.: Development of the Colle-Salvetti correlation-energy formula into a functional of the electron density. *Phys. Rev. B* 37, 785–789 (1988). <https://doi.org/10.1103/PhysRevB.37.785>
- [53] Becke, A.D.: Density-functional thermochemistry. III. The role of exact exchange. *J. Chem. Phys.* 98, 5648–5652 (1993). <https://doi.org/10.1063/1.464913>
- [54] Frisch, M.J. e. al., (see supporting information for full reference).
- [55] Stevens, W.J., Basch, H., Krauss, M.: Compact effective potentials and efficient shared-exponent basis sets for the first- and second-row atoms. *J. Chem. Phys.* 81, 6026–6033 (1984). <https://doi.org/10.1063/1.447604>
- [56] Hay, P.J., Wadt, W.R.: Ab initio effective core potentials for molecular calculations. Potentials for the transition metal atoms Sc to Hg. *J. Chem. Phys.* 82, 270–283 (1985). <https://doi.org/10.1063/1.448799>
- [57] Hay, P.J., Wadt, W.R.: Ab initio effective core potentials for molecular calculations. Potentials for K to Au including the outermost core orbitals. *J. Chem. Phys.* 82, 299–310 (1985). <https://doi.org/10.1063/1.448975>
- [58] Rodgers, M.T., Armentrout, P.B.: Noncovalent Interactions of Nucleic Acid Bases (Uracil, Thymine, and Adenine) with Alkali Metal Ions. Threshold Collision-Induced Dissociation and Theoretical Studies. *J. Am. Chem. Soc.* 122, 8548–8558 (2000). <https://doi.org/10.1021/ja001638d>
- [59] Yang, Z., Rodgers, M.T.: Influence of Halogenation on the Properties of Uracil and Its Noncovalent Interactions with Alkali Metal Ions. Threshold Collision-Induced Dissociation and Theoretical Studies. *J. Am. Chem. Soc.* 126, 16217–16226 (2004). <https://doi.org/10.1021/ja045375p>
- [60] Yang, Z., Rodgers, M.T.: Influence of Thioketo Substitution on the Properties of Uracil and Its Noncovalent Interactions with Alkali Metal Ions: Threshold Collision-Induced Dissociation and Theoretical Studies. *J. Phys. Chem. A* 110, 1455–1468 (2006). <https://doi.org/10.1021/jp054849j>
- [61] Power, B., Haldys, V., Salpin, J., Fridgen, T.D.: Structures of $[M(\text{Ura-H})(\text{Ura})]^+$ and $[M(\text{Ura-H})(\text{H}_2\text{O})_n]^+$ ($M=\text{Cu}, \text{Zn}, \text{Pb}; n=1-3$) complexes in the gas phase by IRMPD spectroscopy in the fingerprint region and theoretical studies. *Int. J. Mass Spectrom.* 429, 56–65 (2018). <https://doi.org/10.1016/j.ijms.2017.05.003>
- [62] Spezia, R., Salpin, J.-Y., Gageot, M.-P., Hase, W.L., Song, K.: Protonated Urea Collision-Induced Dissociation. Comparison of Experiments and Chemical Dynamics Simulations. *J. Phys. Chem. A* 113, 13853–13862 (2009). <https://doi.org/10.1021/jp906482v>

- 1
2
3 [63] Molina, E.R., Ortiz, D., Salpin, J.-Y., Spezia, R.: Elucidating collision induced dissociation products
4 and reaction mechanisms of protonated uracil by coupling chemical dynamics simulations with tandem mass
5 spectrometry experiments. *J. Mass Spectrom.* 50, 1340–1351 (2015). <https://doi.org/10.1002/jms.3704>
6
7 [64] Rossich Molina, E., Salpin, J.-Y., Spezia, R., Martínez-Núñez, E.: On the gas phase fragmentation of
8 protonated uracil: a statistical perspective. *Phys. Chem. Chem. Phys.* 18, 14980–14990 (2016).
9 <https://doi.org/10.1039/C6CP01657J>
10
11 [65] Oomens, J., Sartakov, B.G., Meijer, G., von Helden, G.: Gas-phase infrared multiple photon
12 dissociation spectroscopy of mass-selected molecular ions. *Int. J. Mass Spectrom.* 254, 1–19 (2006).
13 <https://doi.org/10.1016/j.ijms.2006.05.009>
14
15 [66] Macaluso, V., Scuderi, D., Crestoni, M.E., Fornarini, S., Corinti, D., Dalloz, E., Martinez-Nunez, E.,
16 Hase, W.L., Spezia, R.: L-Cysteine Modified by S-Sulfation: Consequence on Fragmentation Processes
17 Elucidated by Tandem Mass Spectrometry and Chemical Dynamics Simulations. *J. Phys. Chem. A* 123,
18 3685–3696 (2019). <https://doi.org/10.1021/acs.jpca.9b01779>
19
20 [67] Fridgen, T.D.: Infrared consequence spectroscopy of gaseous protonated and metal ion cationized
21 complexes. *Mass Spectrom. Rev.* 28, 586–607 (2009). <https://doi.org/10.1002/mas.20224>
22
23 [68] Jašíková, L., Roithová, J.: Infrared Multiphoton Dissociation Spectroscopy with Free-Electron Lasers:
24 On the Road from Small Molecules to Biomolecules. *Chem. - A Eur. J.* 24, 3374–3390 (2018).
25 <https://doi.org/10.1002/chem.201705692>
26
27 [69] Corinti, D., Maccelli, A., Crestoni, M.E., Cesa, S., Quaglio, D., Botta, B., Ingallina, C., Mannina, L.,
28 Tintaru, A., Chiavarino, B., Fornarini, S.: IR ion spectroscopy in a combined approach with MS/MS and IM-
29 MS to discriminate epimeric anthocyanin glycosides (cyanidin 3-O-glucoside and -galactoside). *Int. J. Mass*
30 *Spectrom.* 444, 116179 (2019). <https://doi.org/10.1016/j.ijms.2019.116179>
31
32 [70] Lamsabhi, A.M., Alcamí, M., Mó, O., Yáñez, M.: Gas-Phase Reactivity of Uracil, 2-Thiouracil, 4-
33 Thiouracil, and 2,4-Dithiouracil towards the Cu⁺ Cation: A DFT Study. *ChemPhysChem.* 4, 1011–1016
34 (2003). <https://doi.org/10.1002/cphc.200300704>
35
36 [71] Beck, J.P., Lisy, J.M.: Infrared spectroscopy of hydrated alkali metal cations: Evidence of multiple
37 photon absorption. *J. Chem. Phys.* 135, 044302 (2011). <https://doi.org/10.1063/1.3609760>
38
39 [72] Heine, N., Yacovitch, T.I., Schubert, F., Brieger, C., Neumark, D.M., Asmis, K.R.: Infrared
40 Photodissociation Spectroscopy of Microhydrated Nitrate–Nitric Acid Clusters NO₃ – (HNO₃)_n (H₂O)
41 n. *J. Phys. Chem. A* 118, 7613–7622 (2014). <https://doi.org/10.1021/jp412222q>
42
43 [73] Gregori, B., Guidoni, L., Chiavarino, B., Scuderi, D., Nicol, E., Frison, G., Fornarini, S., Crestoni, M.E.:
44 Vibrational Signatures of S-Nitrosoglutathione as Gaseous, Protonated Species. *J. Phys. Chem. B.* 118,
45 12371–12382 (2014). <https://doi.org/10.1021/jp5072742>
46
47
48
49
50
51
52
53
54
55
56
57
58
59
60

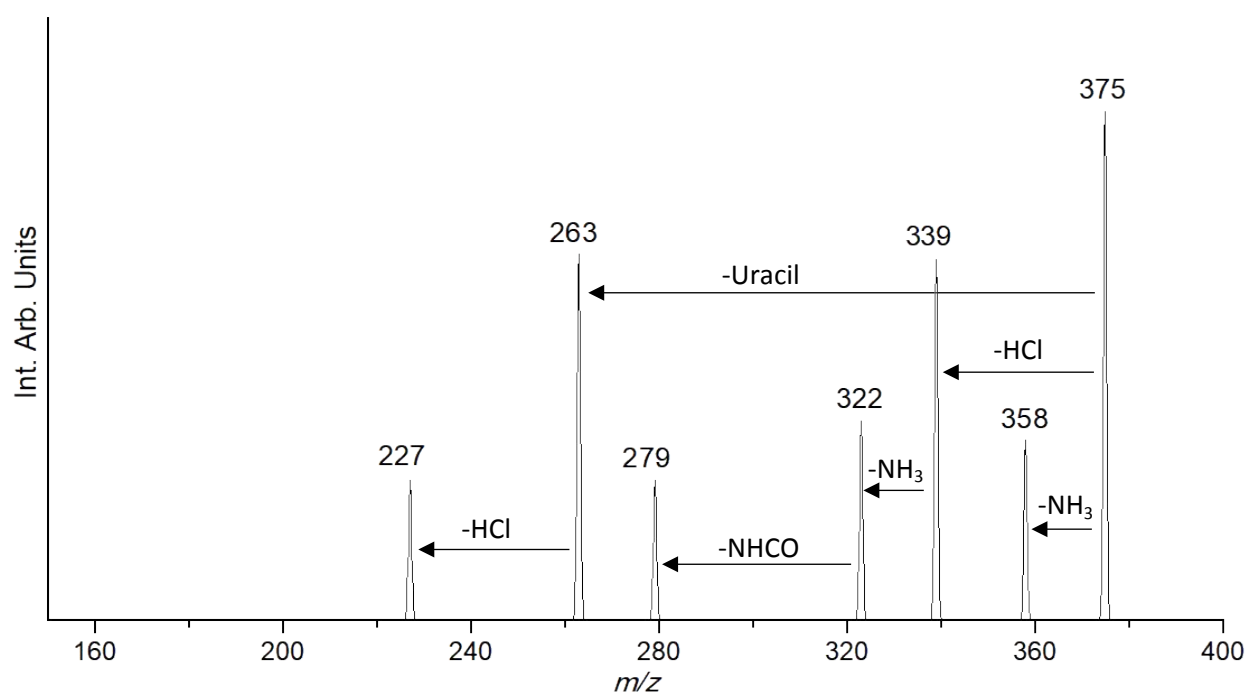


Figure 1. Collision induced dissociation mass spectrum of $\text{cis-}[\text{PtCl}(\text{NH}_3)_2(\text{U})]^+$ at m/z 375 obtained at collision (lab) energy (E_{LAB}) of 5eV in a hybrid triple-quadrupole linear ion trap mass spectrometer (QTrap API 2000). At this E_{LAB} value a considerable fraction of the precursor ion has undergone fragmentation by loss of NH_3 , a process occurring already in the region preceding the collision quadrupole.

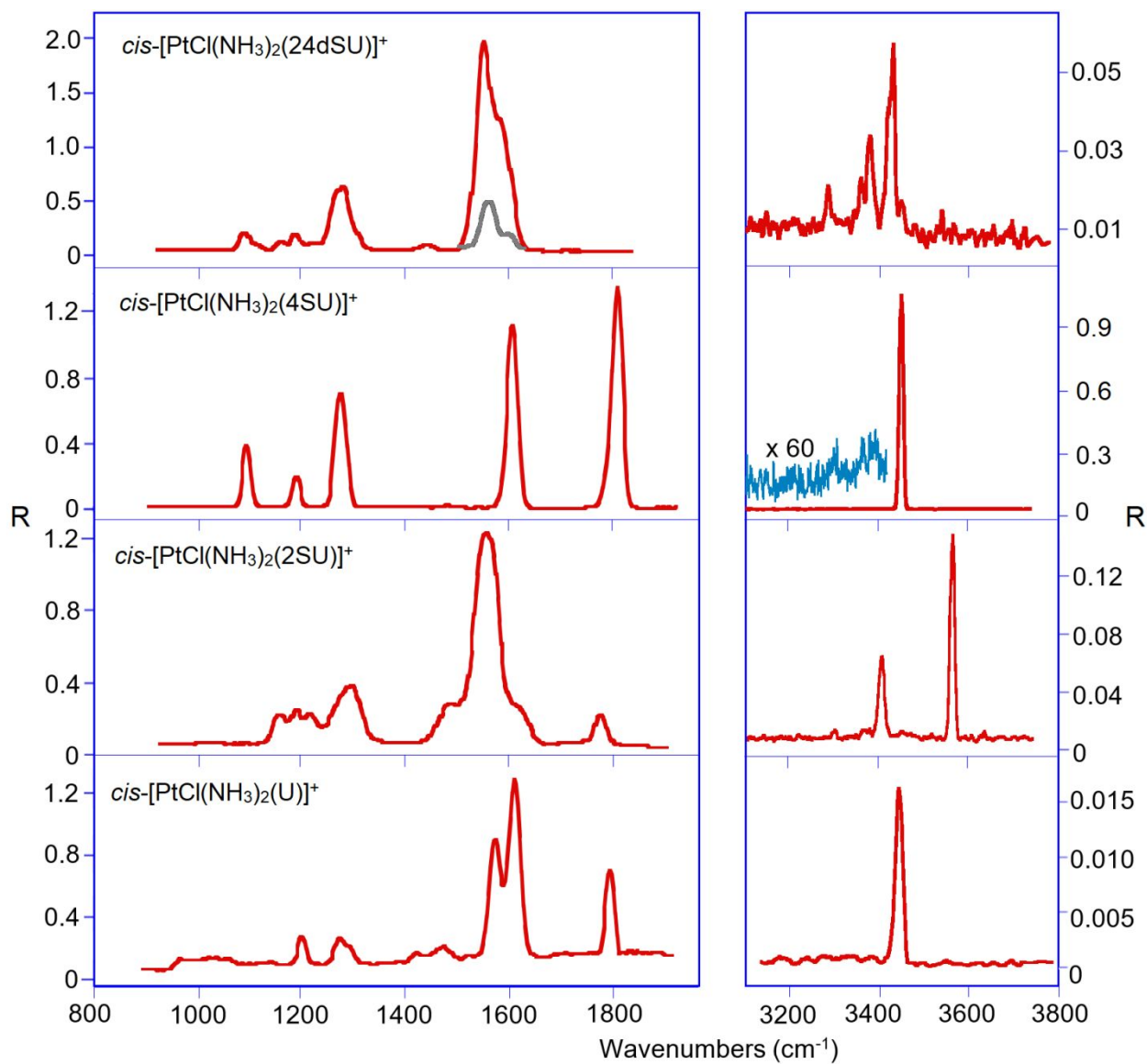


Figure 2. Experimental IRMPD spectra of *cis*-[PtCl(NH₃)₂L]⁺ (from bottom to top L=U, 2SU,4SU, 24dSU) recorded in the fingerprint and in the NH/OH stretch ranges.

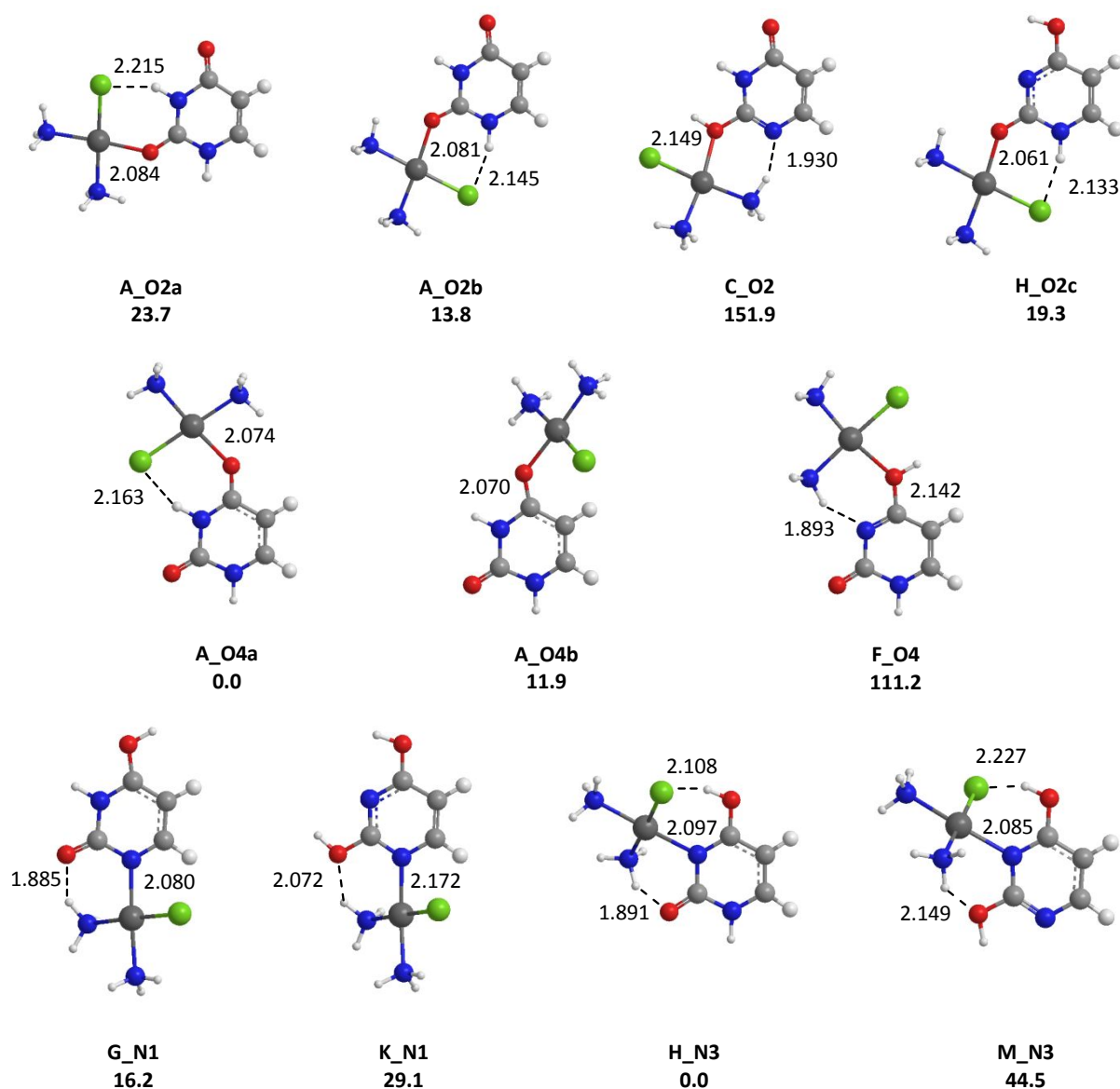
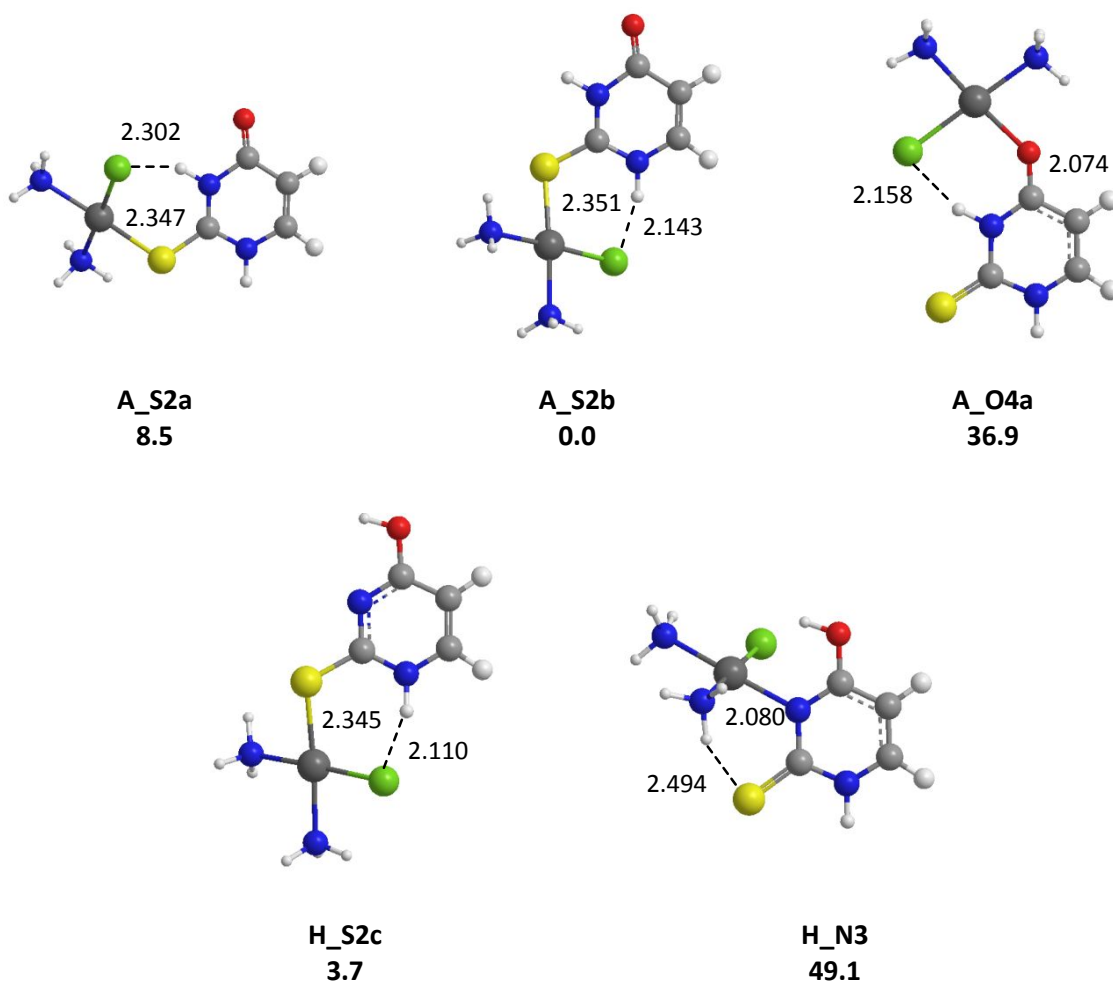
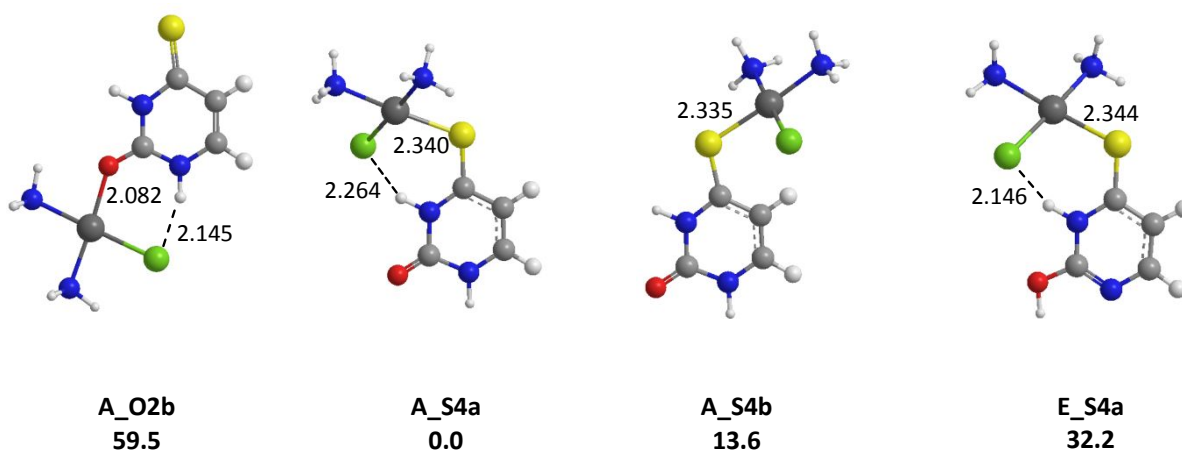


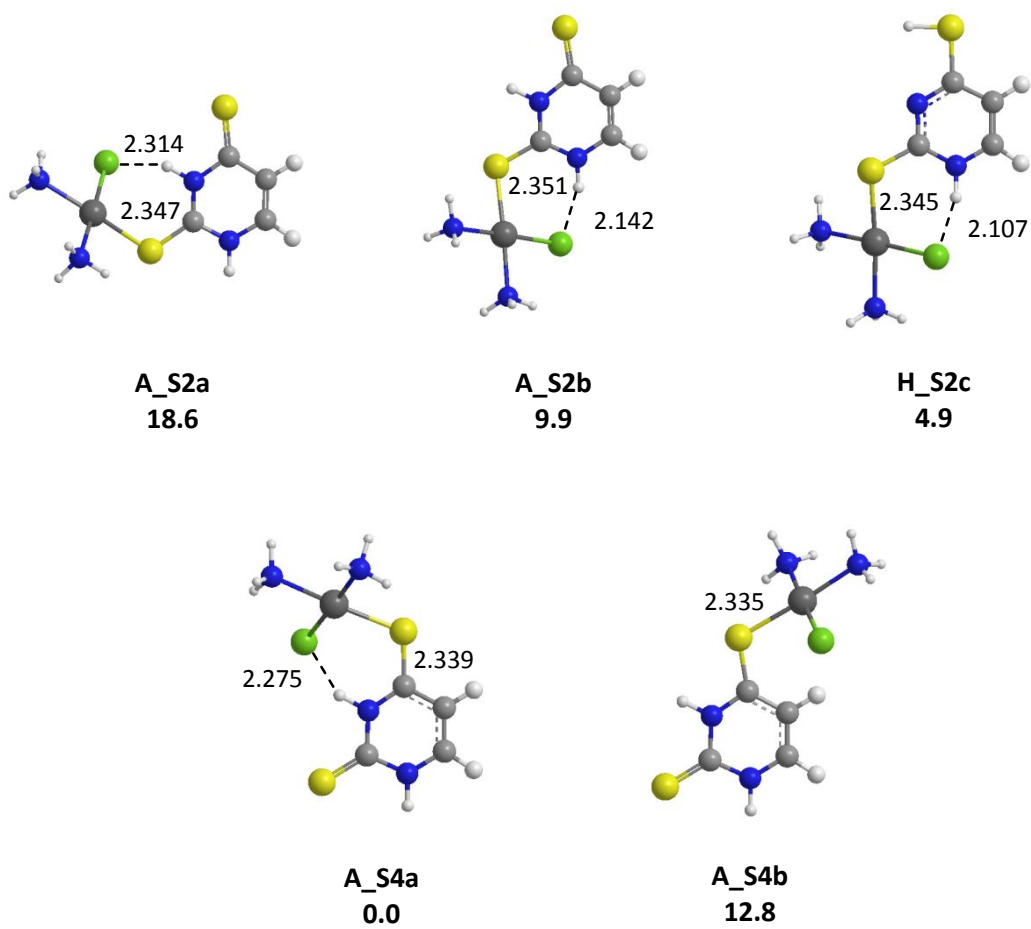
Figure 3. Representative structures obtained for the cis -[PtCl(NH₃)₂(U)]⁺ complexes. B3LYP/LACV3P/6-311G** relative free energies given in kJ/mol. Distances are given in Å.



36 **Figure 4.** Representative structures obtained for the *cis*-[PtCl(NH₃)₂(2SU)]⁺ complexes.
 37 B3LYP/LACV3P/6-311G**relative free energies given in kJ/mol. Distances are given in Å.
 38
 39
 40



56 **Figure 5.** Representative structures obtained for the *cis*-[PtCl(NH₃)₂(4SU)]⁺ complexes.
 57 B3LYP/LACV3P/6-311G**relative free energies given in kJ/mol. Distances are given in Å.
 58
 59
 60



33 **Figure 6.** Representative structures obtained for the *cis*-[PtCl(NH₃)₂(24dSU)]⁺ complexes.
34 B3LYP/LACV3P/6-311G**relative free energies given in kJ/mol. Distances are given in Å.
35
36
37
38
39
40
41
42
43
44
45
46
47
48
49
50
51
52
53
54
55
56
57
58
59
60

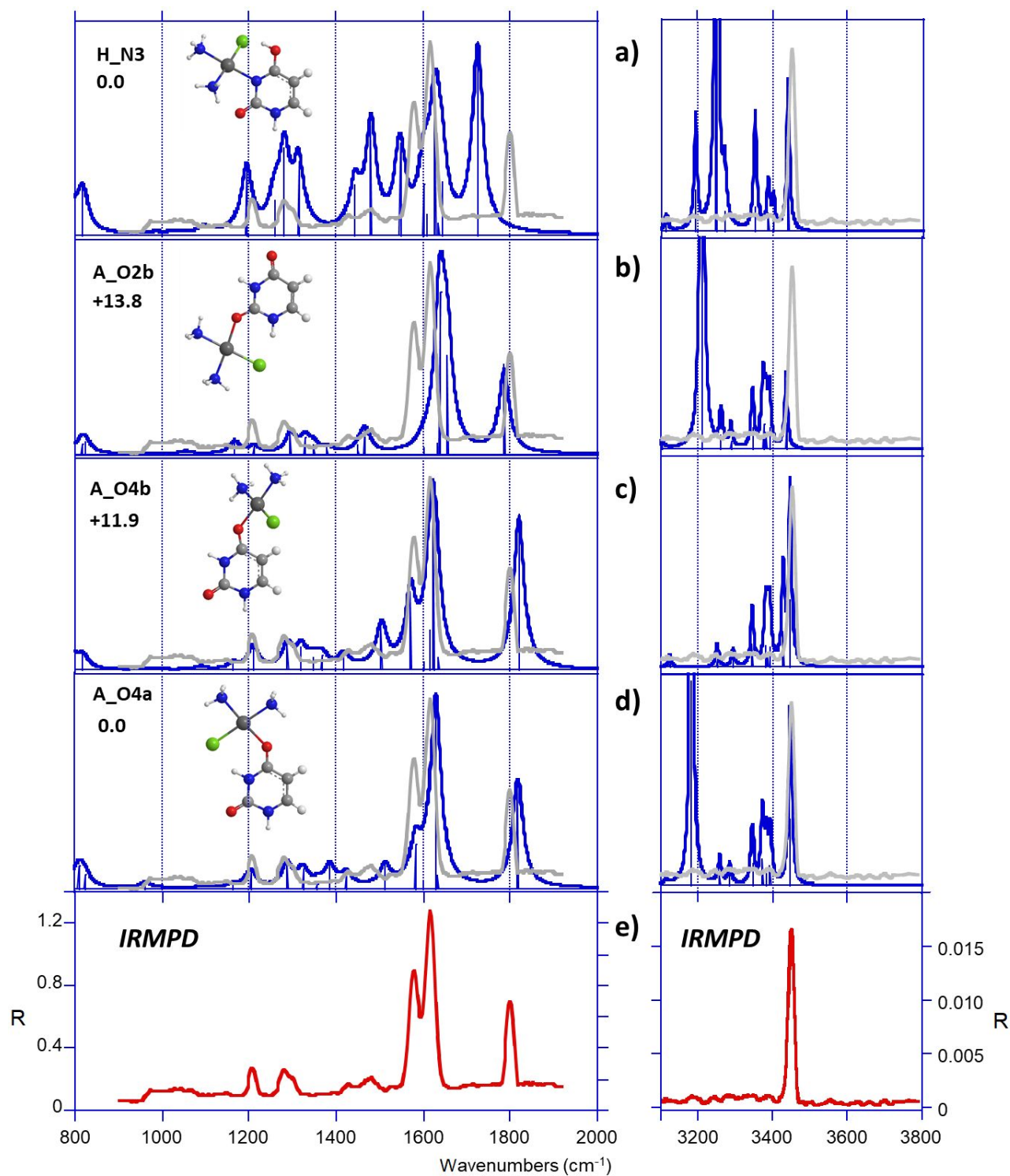


Figure 7. (e) IRMPD spectrum of *cis*-[PtCl(NH₃)₂(U)]⁺ compared with DFT-computed IR absorption spectra (a–d) of some relevant structures. The experimental IRMPD spectrum is overlaid in grey.

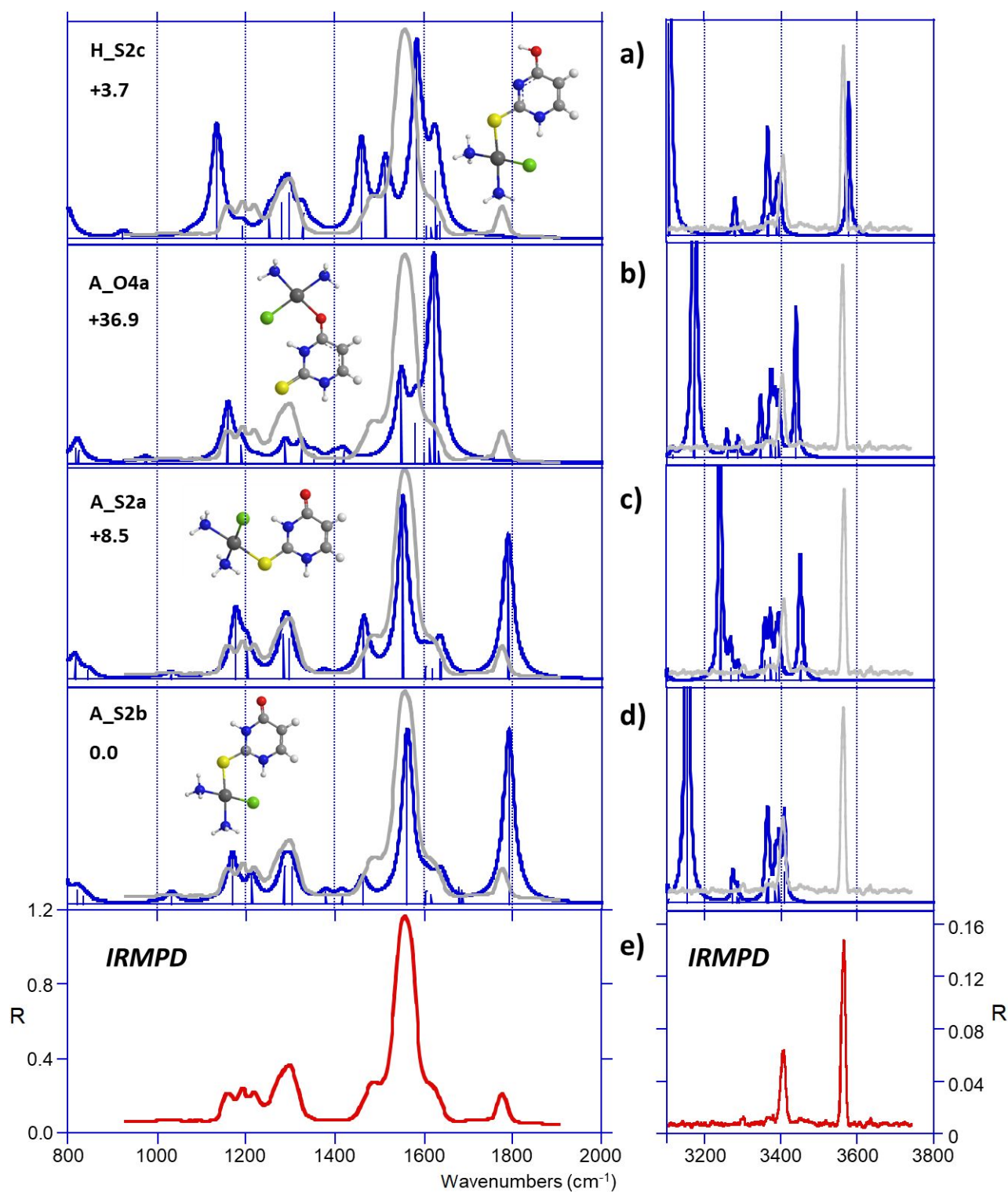


Figure 8. (e) IRMPD spectrum of *cis*-[PtCl(NH₃)₂(2SU)]⁺ compared with DFT-computed IR absorption spectra (a–d) of some relevant structures. The experimental IRMPD spectrum is overlaid in grey.

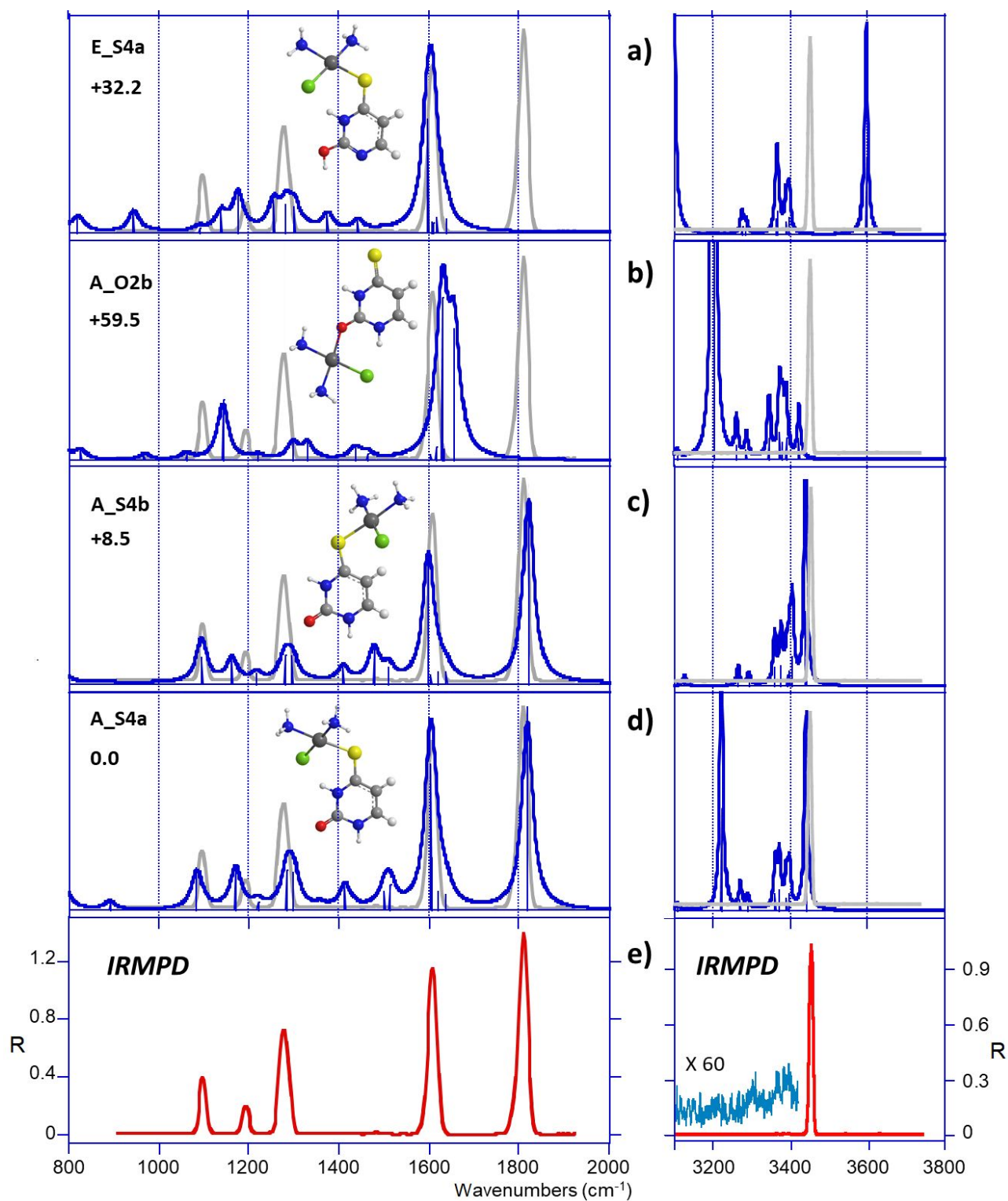


Figure 9. (e) IRMPD spectrum of *cis*-[PtCl(NH₃)₂(4SU)]⁺ compared with DFT-computed IR absorption spectra (a–d) of some relevant structures. The experimental IRMPD spectrum is overlaid in grey.

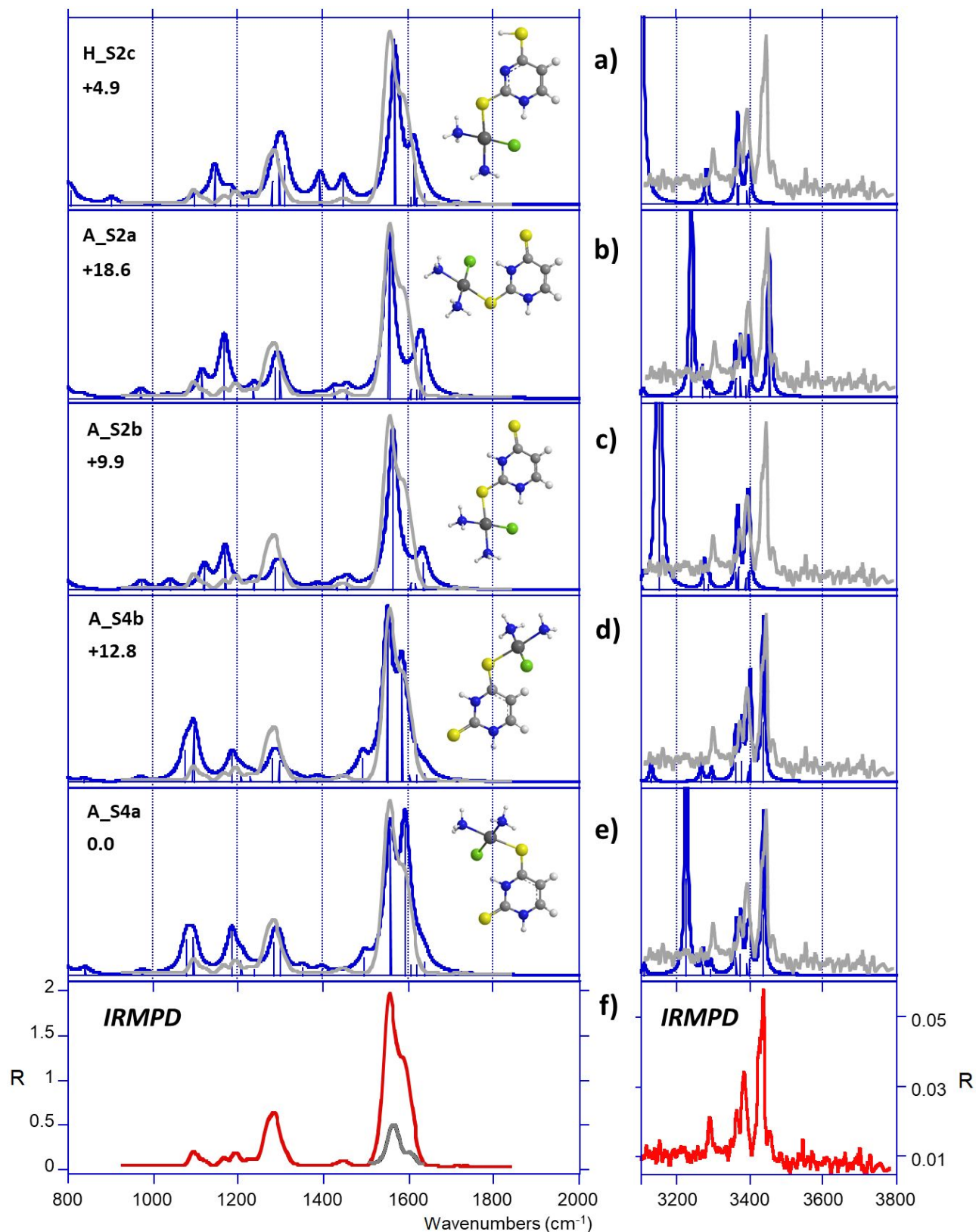


Figure 10. (e) IRMPD spectrum of *cis*-[PtCl(NH₃)₂(24dSU)]⁺ compared with DFT-computed IR absorption spectra (a–d) of some relevant structures. The experimental IRMPD spectrum is overlaid in grey.

Table 1. Observed IRMPD and CID dissociation channels from *cis*-[PtCl(NH₃)₂(L)]⁺ complexes and phenomenological thresholds (kJ mol⁻¹).

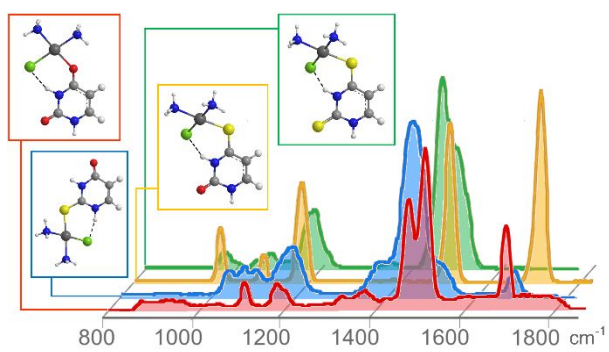
<i>cis</i> -[PtCl(NH ₃) ₂ (L)] ⁺	Reactant ion (m/z)	Product ions ^a (m/z)	Neutral loss	TE ^b
L= U	375	358	NH ₃	n.a. ^c
		339	HCl	
		322	NH ₃ and HCl	
		279	NH ₃ , HCl and NHCO	
		263	U	
		245	U and NH ₃	
		227	U, NH ₃ and HCl	
L= 2SU	391	374	NH ₃	89
		338	NH ₃ and HCl	
		321	2 NH ₃ and HCl	
		295	NH ₃ , HCl and NHCO	
		263	2SU	
L= 4SU	391	374	NH ₃	89
		338	NH ₃ and HCl	
		321	2 NH ₃ and HCl	
		295	NH ₃ , HCl and NHCO	
		263	4SU	
L= 24dSU	407	390	NH ₃	75
		354	NH ₃ and HCl	
		337	2 NH ₃ and HCl	

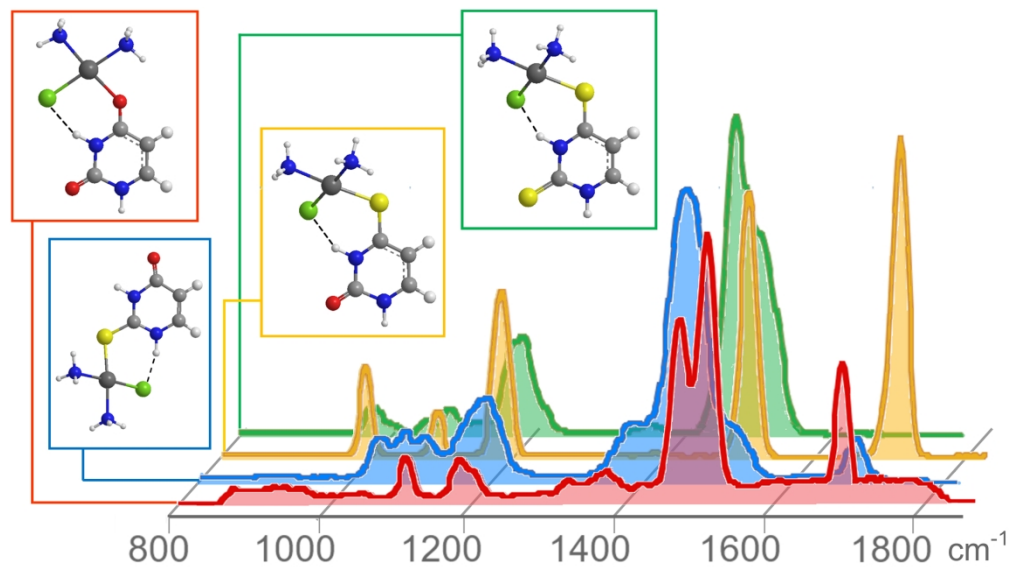
^a Fragments observed only in CID mass spectra are in boldface.

^b Phenomenological threshold energies (TE) in kJ mol⁻¹ are given with ±5-10 kJ mol⁻¹ uncertainty.

^c n.a. stands for not available.

For Table of Contents Only





For Table of Contents only

887x498mm (96 x 96 DPI)